# Simulating Global Terrestrial Carbon and Nitrogen Biogeochemical Cycles with Implicit and Explicit Representations of Soil Microbial Activity

**William R Wieder[1,2*], Melannie D Hartman[1,3], Emily Kyker-Snowman[4], Brooke Eastman[5], Katerina Georgiou[6], Derek Pierson[7], Katherine S Rocci[2,8], A. Stuart Grandy[9,10]**

[1]Climate and Global Dynamics Laboratory, National Center for Atmospheric Research, Boulder, CO

[2]Institute of Arctic and Alpine Research, University of Colorado, Boulder, CO;

[3]Natural Resource Ecology Laboratory, Colorado State University, Fort Collins, CO;

[4]Carbon Direct, New York, NY;

[5]Division of Forestry and Natural Resources, West Virginia University, Morgantown, WV;

[6]Physical and Life Sciences Directorate, Lawrence Livermore National Laboratory, Livermore, CA;

[7]Rocky Mountain Research Station, United States Forest Service, Boise, ID;

[8]Institute for Global Change Biology, University of Michigan, Ann Arbor, MI;

[9]Department of Natural Resources and the Environment, University of New Hampshire, Durham, NH

[10]Center of Soil Biogeochemistry and Microbial Ecology, University of New Hampshire, Durham NH

*Corresponding author: Will Wieder (wwieder@ucar.edu)

**Key Points:**

- Nitrogen limitation of plant productivity increases soil organic matter turnover time with MIMICS-CN
- Higher temperature sensitivity of soil organic matter turnover increases nitrogen mineralization rates
- Soil texture and litter quality affect prognostic soil carbon to nitrogen ratios that are simulated with MIMICS-CN

## Abstract

Nutrient limitation is widespread in terrestrial ecosystems. Accordingly, representations of nitrogen (N) limitation in land models typically dampen rates of terrestrial carbon (C) accrual, compared with C-only simulations. These previous findings, however, rely on soil biogeochemical models that implicitly represent microbial activity and physiology. Here we present results from a biogeochemical model testbed that allows us to investigate how an explicit vs. implicit representation of soil microbial activity, as represented in the MIcrobial-MIneral Carbon Stabilization (MIMICS) and Carnegie–Ames–Stanford Approach (CASA) soil biogeochemical models, respectively, influence plant productivity and terrestrial C and N fluxes at initialization and over the historical period. When forced with common boundary conditions, larger soil C pools simulated by the MIMICS model reflect longer inferred soil organic matter (SOM) turnover times than those simulated by CASA. At steady state, terrestrial ecosystems experience greater N limitation when using the MIMICS-CN model, which also increases the inferred SOM turnover time. Over the historical period, however, higher rates of N mineralization were fueled by warming-induced acceleration of SOM decomposition over high latitude ecosystems in the MIMICS-CN simulation reduce this N limitation, resulting in faster rates of vegetation C accrual. Moreover, as SOM stoichiometry is an emergent property of MIMICS-CN, we highlight opportunities to deepen understanding of sources of persistent SOM and explore its potential sensitivity to environmental change. Our findings underscore the need to improve understanding and representation of plant and microbial resource allocation and competition in land models that represent coupled biogeochemical cycles under global change scenarios.



## Plain Language Summary

Nitrogen limitation of terrestrial ecosystems is common and crates feedbacks between aboveground and belowground biogeochemical cycles. We present a novel analysis looking at how the explicit vs. implicit represention of soil microbial activity influences ecosystem carbon and nitrogen fluxes in a global biogeochemical model. With the microbial explicit model, MIMICS-CN, we found increases in the inferred turnover time of soil organic matter that were caused by plant-soil feeedbacks from nitrogen limitation of plant productivity. Over the historical period, we found that warming-induced acceleration of soil organic matter decomposion resulted in higher rates of nitrogen mineralization and vegetation biomass acurall. Collectively, these findings illustrate the feasibility of simulating global carbon-nitrogen biogeochemical cycles with the explicit representation of microbial decomposers that presents new opportunities to investigate plant-soil interactions.


## 1 Introduction

Terrestrial ecosystems are characterized by widespread nutrient limitation, especially of nitrogen (N; Elser et al., 2007; LeBauer & Treseder, 2008). These limitations fundamentally shape ecosystem feedbacks between above- and belowground processes (Wardle et al., 2004). Plant investment in belowground carbon (C) allocation and nutrient acquisition strategies influences soil biogeochemical cycles, notably through the formation and decomposition of soil organic matter (SOM; Averill et al., 2014). Moreover, microbial biomass is a major driver of nitrogen mineralization rates (Li et al., 2019). Thus, shifting patterns of plant and microbial stoichiometry, allocation, and activity in response to global change drivers will likely influence terrestrial ecosystem responses to climate change (Wieder, Cleveland, et al., 2015; Zaehle et al.,

2015). Accurately capturing these ecological processes and plant-soil feedbacks in models that are used for climate change projections remains a challenge.

Part of this uncertainty reflects gaps in our theoretical understanding of plant-soil feedbacks and their influence on nutrient availability. Notably, emerging theories emphasize the importance of microbial-mineral interactions that govern SOM persistence (Cotrufo et al., 2013; Lehmann et al., 2020; Lehmann & Kleber, 2015). Yet, explicit representations of microbial activity, microbial functional traits, and the protection of soil C via organo-mineral interactions are notably absent from models that are used to project C cycle–climate feedbacks (Todd-Brown et al., 2013). The introduction of global-scale, microbial explicit soil biogeochemical models has opened new lines of research (Ye Huang et al., 2018; Sulman et al., 2014; Wieder et al., 2013; Wieder, Grandy, et al., 2015), but much of the work to date only focuses on the representation of soil C biogeochemistry. Results from ecosystem-scale simulations show the potential for models that explicitly simulate microbial-mineral interactions to advance understanding of coupled carbon-nitrogen (CN) dynamics (Eastman et al., 2023; Kyker-Snowman et al., 2020; Thum et al., 2019; G. Wang et al., 2020; Y. Zhang et al., 2021). Now, application of microbial explicit CN soil models is feasible at global scales (Y. Huang et al., 2021; Sulman et al., 2019), although to date analyses of global terrestrial C and N dynamics from this class of models are sparse.

The current generation of global models consistently show that representing terrestrial nutrient limitation dampens of terrestrial ecosystem responses to elevated $CO_2$ (Thornton et al., 2007; Y. P. Wang et al., 2010; Zaehle et al., 2010). However, these results come from models that implicitly represent soil microbial activity. Preliminary work with models that explicitly represent microbial activity demonstrate shifts in the timing and magnitude of ecosystem C fluxes, relative to models that make microbial implicit assumptions (Basile et al., 2020; Jian et al., 2021; Wieder et al., 2018; Wieder et al., 2019). This suggests that models based on distinct underlying structural assumptions will also generate differences in soil N fluxes that may feedback onto ecosystem productivity and response to global change.

We begin to explore these dynamics by coupling two different soil biogeochemical models that represent C and N biogeochemistry to a common vegetation model. This biogeochemical model testbed allows us to investigate how alternative soil model structures and assumptions ultimately influence plant productivity and ecosystem C storage. This is one of the first global-scale applications of a microbially explicit model to look at ecosystem C and N responses at initialization and in historical simulations (see also Dunne et al., 2020; Sulman et al., 2019). Our objectives are to describe differences in the underlying assumptions of both microbial explicit and microbial implicit model structures that are applied by the MIcrobial-MIneral Carbon Stabilization (MIMICS; Wieder et al., 2014; Wieder, Grandy, et al., 2015) and Carnegie–Ames–Stanford Approach (CASA; Y. P. Wang et al., 2010) soil biogeochemical models, respectively. Subsequently, we describe global scale patterns of soil biogeochemical states and fluxes that are simulated by MIMICS and CASA under steady-state conditions. Finally, we explore the transient biogeochemical response of terrestrial ecosystems over the historical period and discuss future opportunities for representing CN biogeochemistry with microbial explicit structures in land models.

## 2 Materials and Methods

### 2.1 Biogeochemical model testbed and forcing

Simulations presented here build on the C-only version of the biogeochemical model testbed, which couples the CASA vegetation model with the CASA or MIMICS soil biogeochemical models (Wieder et al., 2018; Wieder et al., 2019). Additional developments to represent soil CN biogeochemistry in site-level simulations with MIMICS-CN are provided in Kyker-Snowman et al. (2020). Here we present a global application of MIMICS-CN that connects with representation of vegetation nutrient limitation and soil N transformations that are also applied in CASA-CNP (Y. P. Wang et al., 2010). We compare global-scale results of vegetation and soil pools and fluxes from simulations with C-only and CN configurations of both MIMICS and CASA soil biogeochemical models. As this work builds on an extensive body of literature, including ecosystem scale simulations with the biogeochemical model testbed presented by Eastman et al. (2023), we largely highlight modifications that were implemented in the development and evaluation of global scale simulations with MIMICS-CN in the biogeochemical model testbed.

The biogeochemical model testbed requires daily inputs of gross primary production (GPP), air temperature, soil temperature, and soil moisture. We generated these boundary conditions by running a historical simulation of the Community Land Model, version 5, with satellite phenology (CLM5-SP) that was driven with atmospheric forcing from the Global Soil Wetness Program, version 3 (GSWP3, see Lawrence et al., 2019). Our previous work with the biogeochemical model testbed used an older version of CLM (version 4.5) and CRU-NCEP forcing (Wieder et al., 2018). Comparison of CLM model versions and forcing data are described in Lawrence et al. (2019) and Bonan et al. (2019). Daily history files from the nominal two degree-resolution CLM5-SP simulations were processed to generate the required meteorological forcings, or *met* files, that are needed to run the biogeochemical model testbed (see technical documentation in Wieder et al., 2023). This processing step involves calculating depth weighted mean daily soil temperature along with volumetric liquid and frozen soil water content for the top six soil layers that are simulated by CLM5 (roughly corresponding to 0-50 cm depth). The *met* files also include daily GPP, air temperature, and N deposition that are simulated by CLM5 and required to run CASA-CNP. Additional input data needed to run the biogeochemical model testbed include soil texture (sand and clay fraction) and dominant plant functional type (PFT) distributions, which are also taken from CLM5 surface datasets.

Initial conditions in the biogeochemical model testbed were generated by spinning up vegetation and soil C pools by cycling over simulation years from (1901-1920) until steady-state conditions were reached. We did this in four model experiments: for C-only and CN versions of both MIMICS and CASA that were coupled to the CASA vegetation model. GPP was identical in all four of these simulations. Net primary production (NPP) and litterfall fluxes were identical for both of the MIMICS and CASA C-only simulations, reflecting autotrophic respiration parameterizations in the C-only CASA vegetation model. Nitrogen limitation of NPP, however, reduced litterfall fluxes in the CN experiments – reflecting differences in the N limitation experienced by plants, given the feedback from different soil biogeochemical models. The CASA vegetation model increases autotrophic respiration fluxes, thereby reducing NPP, when daily inorganic N pools are less than 1g N $m^{-2}$. Differences in steady-state initial conditions are described in section 3.1. Subsequently we ran transient simulations over the historical period

from 1901-2014 for each of our four model experiments, with results described in section 3.2. We did not run the biogeochemical model testbed with transient land use or land cover change.

## 2.2 MIMICS-CN

In this section we describe highlights of this global-scale implementation of CN biogeochemistry in MIMICS and provide relevant information about underlying assumptions and approaches taken in the MIMICS and CASA soil models. Notable features of MIMICS include the representation of metabolic and structural litter pools ($LIT_m$ and $LIT_s$), explicit representation of fast and slow growing microbial functional groups ($MIC_r$ and $MIC_K$), and the representation of physicochemically protected, chemically protected, and available soil organic matter pools ($SOM_p$, $SOM_c$, and $SOM_a$; Figure 1). The basic structure of the model has not been changed from the C-only version of MIMICS (Wieder et al. 2015) with addition of CN biogeochemistry described in Kyker-Snowman et al. (2020) and Eastman et al. (2023). As in our previous work (Wieder et al., 2018; Wieder et al., 2019), MIMICS-CN uses temperature-sensitive reverse Michaelis-Menten kinetics to describe microbial community catabolic capacity (blue lines, Fig 1), which determine rates of litter and SOM decomposition that are modified by soil liquid water availability. MIMICS-CN also represents microbial growth efficiency that controls the fate of C and N fluxes in soils through microbial carbon use efficiency, nitrogen use efficiency, and microbial turnover (CUE, NUE, and **τ**, respectively; green lines, Fig. 1), which are a function of substrate quality and microbial functional groups. Microbial necromass fluxes from each microbial functional group are allocated to different SOM pools, which vary as a function of soil clay content and litter quality (orange lines, Fig. 1). Litter quality determines allocation of microbial residues ($f_c$) that enter the chemically protected ($SOM_c$) pool. Soil clay content controls allocation to and turnover ($f_p$ and D, respectively) of the physicochemically protected ($SOM_p$) pool in MIMICS.

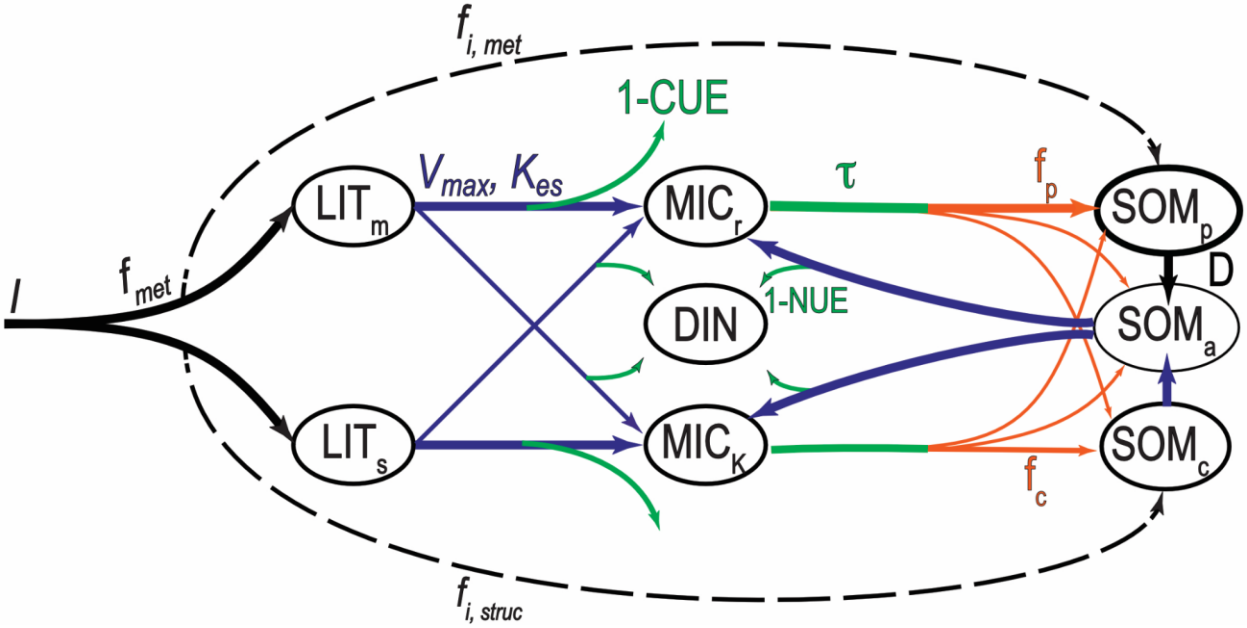


**Figure 1.** Pools of litter, microbial biomass and soil organic matter (LIT, MIC, and SOM, respectively) that are represented in MIMICS-CN. Microbial catabolic potential (blue lines) varies with daily soil temperature and soil moisture and drives the decomposition of litter and

soil organic matter. Microbial growth rates (green lines) are determined by carbon use efficiency, nitrogen use efficiency, and turnover (CUE, NUE and **τ**). CUE and NUE contribute to heterotrophic respiration and nitrogen mineralization fluxes, which occur for all fluxes into microbial biomass pools (but are not shown for clarity). Microbial necromass is partitioned into SOM pools as a function of soil clay content and litter quality (orange lines).

Litterfall inputs (I) in MIMICS and CASA are partitioned into litter pools based on chemical quality, specifically the weighted average lignin:N ratio of all litter inputs determines the fraction of metabolic litter ($f_{MET}$) as in Parton et al. (1987) and applied by Wieder et al. (2014). One notable difference, however, is that fluxes from the decay of coarse woody debris are transferred into structural litter pools in MIMICS, thus the lignin:N ratio associated with this flux is also included in the calculation of $f_{MET}$. By contrast, fluxes of coarse woody debris in CASA are transferred directly to SOM pools and, therefore, not included in the CASA calculation of $f_{MET}$. In MIMICS-CN we hold the stoichiometry of the metabolic litter inputs (and therefore the $LIT_m$ pool) constant, assuming that this relatively labile litter flux has a high chemical quality (C:N = 15). Thus, the C:N of structural litter inputs (and the $LIT_s$ pool) varies to conserve total N inputs from litterfall (Kyker-Snowman et al., 2020). A fraction of litter inputs bypasses the litter, and therefore microbial biomass pools, in MIMICS ($f_i$, Figure 1). The current parameterization of the model assumes a larger fraction of low quality, structural litter inputs are passed directly to the chemically protected SOM pool, which we think of as being analogous to a particulate organic matter pool (POM; $f_{i,\,struc}$ = 0.3, or 30% of structural litter inputs). By contrast, relatively little metabolic litter directly contributes to the formation of physicochemically protected SOM, which we consider to be more like a mineral associated organic matter pool (MAOM; $f_{i,\,met}$ = 0.005, or 0.5% of metabolic litter fluxes). This change was made with the representation of N biogeochemistry in MIMICS-CN for site-level simulations by Kyker-Snowman et al. (2020) to increase the C:N ratio of bulk SOM pools, and also applied for global scale MIMICS C-only and CN runs presented here. Lower input rates and turnover times to $SOM_p$ pools were also implemented in the parameterization of MIMICS-CN presented here to achieve longer turnover times of this MAOM-like pool (Pierson et al., 2022; Wieder et al., 2019; H. Zhang et al., 2020).

The microbial functional groups represented in MIMICS are intended to represent functional trait tradeoffs between microbial growth rates (blue lines in Fig 1) and microbial growth efficiency and turnover (green lines in Fig. 1) (Joshua P. Schimel & Schaeffer, 2012; Wieder et al., 2014). The model parameters reflect assumptions that a fast-growing microbial functional group ($MIC_r$) has a greater affinity for organic matter substrates with higher chemical quality ($LIT_m$) but has a lower CUE than a slower growing microbial functional group ($MIC_K$), which has a greater affinity for low chemical quality substrates ($LIT_s$) (Wieder et al., 2018).

Microbial stoichiometry in MIMICS-CN builds on this functional trait framework. We assumed that the higher catabolic potential ($V_{max}$) of $MIC_r$ communities requires more nitrogen, resulting in lower microbial biomass C:N ratios, compared to slower growing copiotrophs. Kyker-Snowman et al. (2020) assign fixed C:N ratios for $MIC_r$ and $MIC_K$ – 6 and 10 respectively, which generally reflects the mean C:N stoichiometry of bacteria and fungi (Cleveland & Liptzin, 2007). Total microbial biomass stoichiometry, therefore, reflects the relative abundance of these functional groups. Preliminary results using this approach in the biogeochemical model testbed, however, produced relatively constrained estimates for ecosystem microbial C:N ratios, compared to results from cross-biome syntheses (Cleveland &

Liptzin, 2007)and subsequent global extrapolations (Gao et al., 2022; Xu et al., 2013). Substrate quality, however, influences microbial community composition and stoichiometry (N. Fanin et al., 2013; Nicolas Fanin et al., 2014; Nemergut et al., 2010). Thus, we developed a simple parameterization that modifies the target microbial biomass stoichiometry as a function of litter quality (eq. 1)

$$CN_{target} = CN_{base} \sqrt{(CN_{mod}/f_{MET})} \quad eq.1$$

Where the target CN ratio is the product of the base C:N ratio for copiotrophs and oligotrophs (6 and 10, respectively) and an empirical function using a CN modifier term (0.4 for these simulations) and $f_{MET}$ (from litterfall inputs, Fig 1). This parameterization allows for somewhat greater spatial variability in microbial C:N ratios and is applied in the results presented here. Accordingly, the emergent microbial biomass stoichiometry that is simulated by MIMICS still reflects the relative abundance of microbial functional groups, but also the influences of litter quality.

Heterotrophic respiration fluxes in MIMICS are determined by the fluxes of C entering microbial biomass pools and associated CUE (Fig 1). In MIMICS, CUE varies by microbial functional group (higher for $MIC_K$ than $MIC_r$, with a particular substrate) and substrate quality (e.g., $LIT_m$ has a higher CUE than $LIT_s$ for a given microbial functional group) (see technical documentation Wieder et al., 2023). We assume that 'messy eating' results in a 85% NUE on fluxes entering microbial biomass pools, with the remaining 15% of decomposed organic N being transferred to the dissolved inorganic nitrogen pool (DIN; models in the testbed do not simulate individual pools of ammonium and nitrate).

After accounting for these C and N losses from donor pool fluxes (coming from $LIT_m$, $LIT_s$, or $SOM_a$), MIMICS-CN evaluates the stoichiometry of incoming fluxes to the receiver pools (going to $MIC_r$ or $MIC_K$) and their target stoichiometry. If the C:N ratio of total fluxes into microbial biomass pools is lower than their respective target, then this excess N is mineralized into the DIN pools. Conversely, if the C:N ratio of inputs to microbial biomass pools is higher than their respective targets then overflow respiration occurs, with this excess C added to the heterotrophic respiration flux. With the current model parameterization, microbial functional groups in MIMICS-CN are not generally C limited, which is generally consistent with empirical measurements and theoretical understanding (Soong et al., 2020), so overflow respiration fluxes are very small. Thus, in MIMICS-CN decomposition of litter and SOM pools proceeds independent from the size of the inorganic N pool. This approach differs from assumptions in the CASA soil biogeochemical model, which downregulates heterotrophic activity if inorganic N pools are < 1gN $m^{-2}$ (Y. P. Wang et al., 2010). Similar assumptions are made in other soil biogeochemical models that downregulate decomposition rates under nitrogen limitation (Bonan et al., 2013; Thomas et al., 2015).

### 2.3 Analyses

We inferred soil C turnover times as the ratio of total soil C stocks and NPP simulated by the models at each grid cell at initialization (1901-1920 mean) (Koven et al., 2017). To compare inferred soil C turnover times between CN and C-only versions of both soil biogeochemical models we calculated response ratios, which were calculated as the natural log of the quotient of results from the CN and C-only versions of MIMICS and CASA; thus, response ratios of 0 signify that the CN and C-only versions of the model are identical. We assessed N limitation as

the difference of NPP from CN and C-only simulations, such that more negative values reflect greater N limitation. We calculated net ecosystem production (NEP) as the difference of GPP and ecosystem respiration fluxes; thus positive values of NEP values reflect net land C uptake. By definition NEP is zero under steady-state, initial conditions.

We compared the latitudinal distribution and global sums for soil biogeochemical states and fluxes that were simulated by MIMICS and CASA with globally gridded estimates from database products. Specifically, we included total soil C stocks for 0-1 m depth from the Harmonized World Soils Database, version 1.2 (HWSD; FAO et al., 2012) that was regridded to a nominal 1 degree resolution (Wieder et al 2014), Soil Grids, version 2.0 (Poggio et al., 2021; 500m resolution was also regridded to a nominal 1 degree resolution), and the Northern Circumpolar Soil Carbon Database (NCSCD; Hugelius et al., 2013). We also compared microbial C and microbial C:N estimates from Xu et al. (2013); (see also Xu et al., 2014) and Serna-Chavez et al. (2013), heterotrophic respiration fluxes derived by Hashimoto et al. (2015), and soil C:N derived from the ratio of organic C and total N (0-1 m depth) from the Global Soil Dataset for use in Earth System Models (GSDE; Shangguan et al., 2014). We note that we are comparing steady state model results, intended to represent conditions at the start of the 20th century (1901-1920 mean state), with observations that are intended to be more representative of contemporary conditions. For slow turnover pools like bulk SOM, we feel the latitudinal patterns we present are unlikely to have appreciably changed over the historical period, but acknowledge that microbial biomass and heterotrophic respiration are likely changing more rapidly.

## 3 Results

### 3.1 Initial conditions

For initialization, all simulations received identical fluxes of GPP (106 Pg C $y^{-1}$, global mean 1901-1920; Table 1). Lower NPP fluxes in MIMICS-CN and CASA-CN simulations reflect N limitation on plant growth, relative to the C-only simulations. MIMICS-CN simulated greater N-limitation in boreal forests (Figure S1), and had slightly lower NPP globally than results from CASA-CN (Table 1). With lower NPP and subsequent litterfall fluxes, steady-state soil C pools were also lower for CN versions of MIMICS and CASA than soil C stocks in each models' C-only counterpart. Initial global soil C stocks simulated by MIMICS totaled 1516 and 1582 Pg C (for CN and C-only simulations, respectively, including the sum of all litter, microbial biomass and soil C pools at 0-100 cm depth; Table 1). Initial soil C stocks simulated by CASA totaled 887 and 997 Pg C (again for CN and C-only simulations, respectively, Table 1).

**Table 1.** Summary of annual fluxes and states simulated by MIMICS and CASA models with CN and C- only biogeochemistry at initialization. Values represent globally integrated means of annual data simulated from 1901-1920. By definition, soil heterotrophic respiration fluxes (HR) are equal to net primary production (NPP) at initialization. Total soil C includes all litter, microbial biomass and soil carbon pools simulated by the models. Relative microbial biomass is the fraction of the total soil C pool composed of microbial biomass and is shown as the global mean across all vegetated grid cells. Similarly, total soil C:N and microbial biomass C:N reflect global means for these quantities.

| | **MIMICS-CN** | **MIMICS C-only** | **CASA-CN** | **CASA C-only** |
|---|---|---|---|---|
| **GPP (Pg C $y^{-1}$)** | 106 | 106 | 106 | 106 |
| **NPP (Pg C $y^{-1}$)** | 38.2 | 42.0 | 38.9 | 42.0 |
| **HR (Pg C $y^{-1}$)** | 38.2 | 42.0 | 38.9 | 42.0 |
| **Total soil C (Pg C)** | 1516 | 1582 | 887 | 997 |
| **Total vegetation C (Pg C)** | 287 | 333 | 298 | 333 |
| **Microbial biomass (Pg C)** | 13.4 | 14.8 | - | - |
| **Relative microbial biomass C (%)** | 0.88 | 0.92 | - | - |
| **Net N mineralization (Tg N $y^{-1}$)** | 876 | - | 888 | - |
| **Total soil C:N** | 11.8 | - | 18.5 | - |
| **Microbial C:N** | 6.8 | - | - | - |

Larger soil C pools in MIMICS-CN reflect longer inferred soil carbon turnover times than those simulated by CASA-CN (Fig. 2a). Similar results were reported for the C-only versions of these models (Wieder et al., 2018) and reflect parametric and structural differences between the MIMICS and CASA soil biogeochemical models. The apparent banding in CASA simulations (Fig. 2a) result from biome-specific soil C turnover times of slow and passive soil C pools, including notably rapid turnover times in agricultural soils (Y. P. Wang et al., 2010). MIMICS does not share this feature. Instead, longer turnover times simulated by MIMICS emerge from a common, global parameterization of the model.

The representation of CN biogeochemistry does not meaningfully alter soil C turnover times that are simulated by CASA-CN, but it does in MIMICS (Fig. 2b). In colder and drier biomes that are less productive, soil C turnover times increase in MIMICS-CN, relative to the C-

only version of the model. Since N limitation of NPP reduces litterfall fluxes, it also reduces the size of the microbial biomass pool in MIMICS-CN (Table 1). The response ratios of microbial biomass and inferred turnover times with MIMICS-CN show a strong, negative linear correlation (Fig. 2c). Thus, longer soil C turnover times in MIMICS-CN resulted from N limitation of plant production that reduced microbial biomass pools and slowed turnover times, especially across high latitude ecosystems (Fig. 2d).

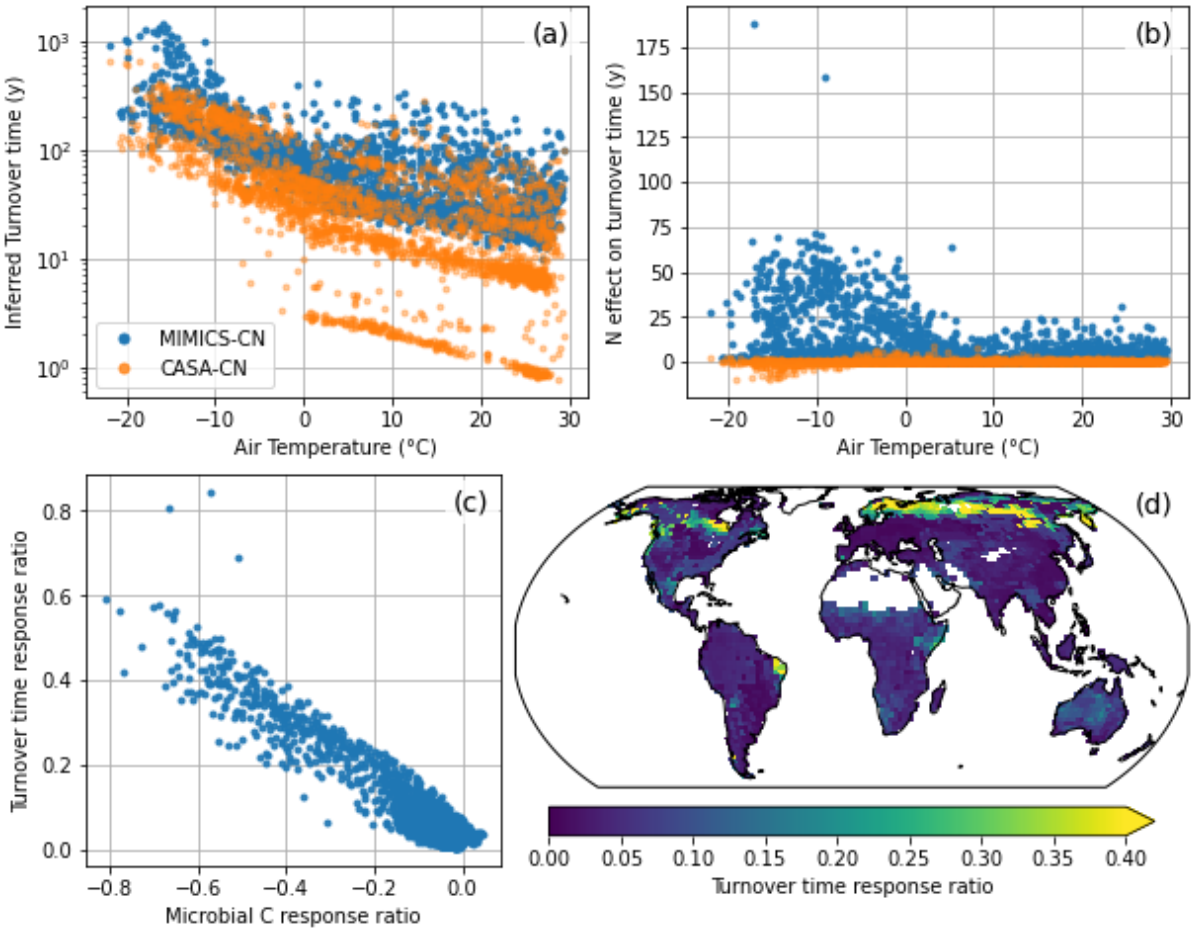


**Figure 2**. Inferred soil C turnover times as a function of mean annual air temperature (**a**) for all grid cells for MIMICS-CN and CASA-CN simulations (blue & orange points, respectively) and (**b**) the difference in turnover times in CN configurations compared to the C-only versions of each model. Soil C turnover is calculated as the ratio of total soil C stocks and NPP simulated by the models at initialization (1901-1920 mean). In MIMICS (**c**) the microbial biomass C response ratio in each grid cell is negatively correlated with the soil C turnover time response ratio. The (**d**) soil C turnover time response ratio in MIMICS-CN is greatest in high-latitude ecosystems that also show stronger N limitation of NPP.

All models (C-only and CN versions of CASA and MIMICS) show latitudinal distributions of soil C stocks that agree reasonably well with observationally derived estimates (Fig. 3a) and global soil C stocks to 1 m depth (1690 Pg C from SoilGrids and 1260 Pg C for the HWSD; Table 1). Microbial biomass carbon totals 13.1 and 14.8 Pg C globally in the CN and C-only versions of MIMICS (Table 1). Global extrapolations from observational syntheses estimate

microbial biomass C ranging from 14.6 to 23.2 Pg C (0-100 cm depth; Serna-Chavez et al., 2013; Xu et al., 2013). Both versions of MIMICS simulate larger microbial biomass pools in high latitude ecosystems, which fall within the large uncertainty from observationally upscaled estimates (Fig. 3b). Globally, relative microbial biomass C (microbial C as a percent of total soil C stocks) is roughly 0.9% in MIMICS (Table 1), which is lower than observationally derived estimates of 1.2% from Serna-Chavez et al. 2013 (Fig. 3c). Notably, MIMICS simulates larger relative microbial biomass pools in temperate and tropical forests and smaller relative microbial biomass pools in arid regions and boreal forests. While these patterns agree with observational estimates, spatial biases persist, especially in temperate and tropical forests (Fig. 3c). Heterotrophic respiration fluxes that are simulated by MIMICS and CASA generally match latitudinal patterns from database estimates reported by Hashimoto et al. (2015; Fig. 3d). At steady state, heterotrophic respiration fluxes are equal to NPP (Table 1). As such, this observational target provides more information about the quality of input data (here GPP derived from CLM and subsequent NPP calculated by the CASA vegetation model) than it does about heterotrophic respiration fluxes that are simulated by any of the soil biogeochemical models.

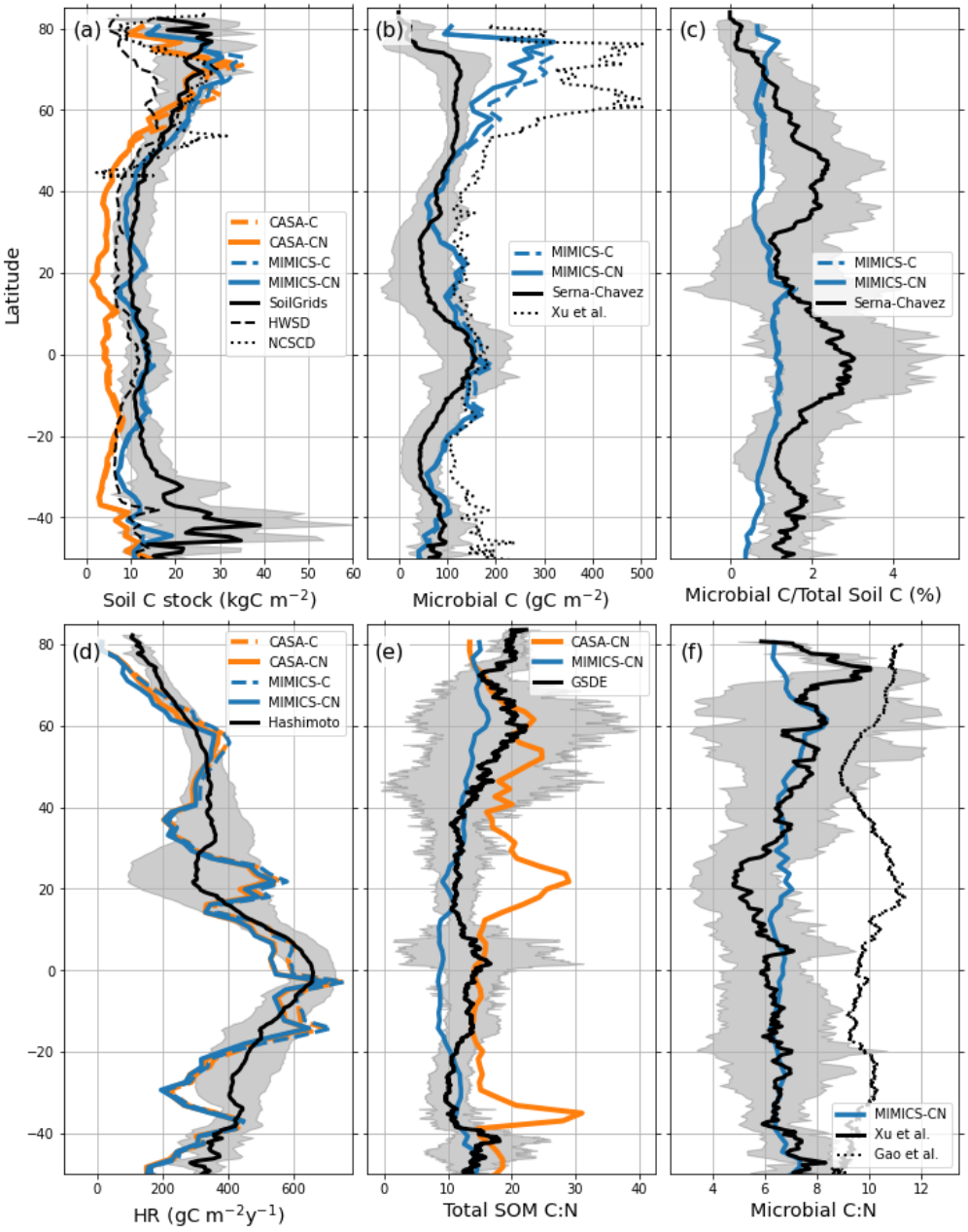


**Figure 3**. Zonal mean plots for MIMICS and CASA simulations (blue and orange lines, respectively) with coupled CN biogeochemistry and C-only configuration (solid and dashed lines, respectively) and relevant observations (black lines with gray shading showing +/- 1 standard deviation of mean). Panels show (**a**) soil C stocks (kgC m$^{-2}$, 0-100 cm depth), (**b**) soil microbial biomass C stocks (gC m$^{-2}$, 0-100 cm depth), (**c**) relative microbial biomass C (microbial C as a percent of total soil C stocks) (**d**) soil heterotrophic respiration fluxes (gC m$^{-2}$ y$^{-1}$), (**e**) soil organic matter C:N ratio, and (**f**) microbial biomass C:N ratios. See methods for references of observations used in this analysis.

Soil stoichiometry is prescribed for each plant functional type in CASA-CN, which produces high soil C:N ratios in semi-tropic, arid regions (Fig 3e). By contrast, the soil

stoichiometry simulated by MIMICS-CN is an emergent property of the model. Both models demonstrate a relatively good match with global observations from Shangguan et al. (2014; Fig. 3e), although MIMICS-CN underestimates soil C:N ratios across boreal forests and, to a lesser extent, in the tropics. MIMICS-CN predicts a latitudinal gradient in soil stoichiometry that largely reflects differences in microbial biomass and litterfall stoichiometry (Fig. 4). Microbial biomass stoichiometry in MIMICS-CN is flexible within narrow ranges (see methods), but is also dependent on the relative abundance of microbial functional types (fast vs. slow). This approach produces global estimates of microbial C:N ratios of 6.8 (Table 1), which are close to observationally based upscaled estimates reported by Xu et al. (2013; global mean microbial C:N = 7.6), but lower than estimates from Gao et al. (2022; global mean microbial C:N = 10; Fig. 3f).

The C:N ratio of SOM, microbial biomass, and litterfall fluxes that are simulated by MIMICS-CN are highest in boreal forests and lower in the tropics, especially in grassland and savanna regions (Fig. 4a-c). The stoichiometry of litter inputs as well as soil moisture control the relative abundance of fast vs. slow microbial functional groups in the model. Accordingly, forests and arid regions tend to have a lower relative abundance of fast growing, copiotrophic microbes (Fig. 4d).

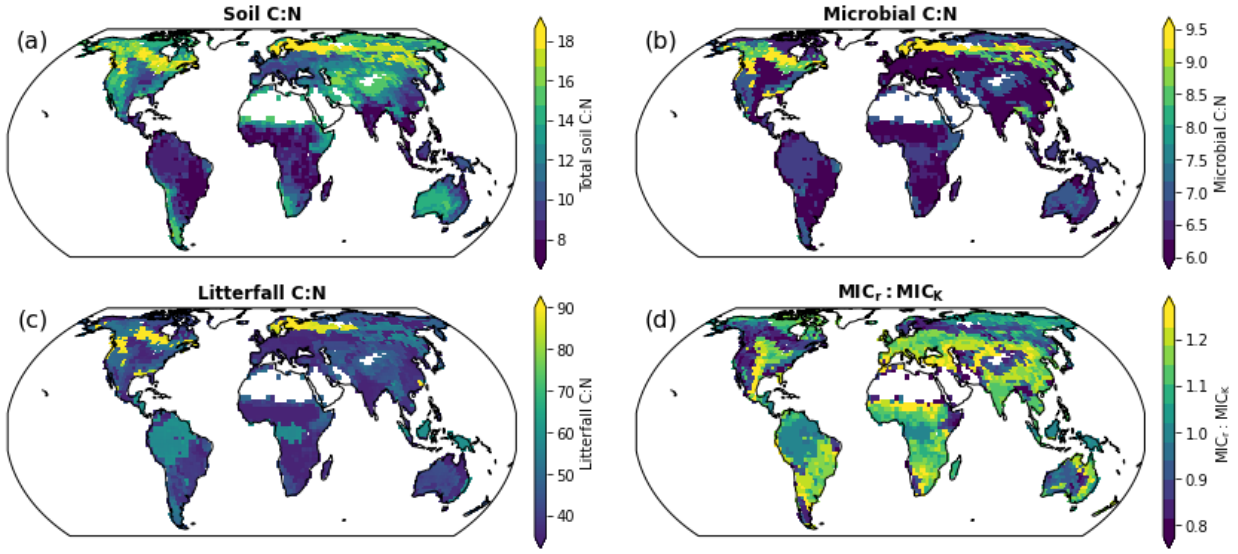


**Figure 4.** Spatial distribution of mean (**a**) soil C:N, (**b**) microbial biomass C:N, (**c**) litterfall C:N, and (**d**) the relative abundance of $MIC_r$:$MIC_K$ that were simulated by MIMICS-CN at initialization (1901-1920).

Soil texture and litter stoichiometry interact to determine the soil C:N ratios that are simulated by MIMICS-CN (Fig. 5). For a given litter quality, higher clay fraction results in lower soil C:N ratios. For a given clay fraction, decreasing litter quality (higher litterfall C:N ratios) results in higher soil C:N ratios that are simulated by MIMICS. Both of these occur in MIMICS because increasing litter quality and clay content also increase the fraction of SOM that persists in the physicochemically protected SOM pool of the model ($SOM_p$). By contrast, CASA-CN parameterized soil stoichiometry based on plant functional type, resulting in higher soil C:N ratios than those simulated by MIMICS-CN (Fig. 3e), but without evidence of the soil properties and litter quality effects on SOM stoichiometry (Fig 5b).

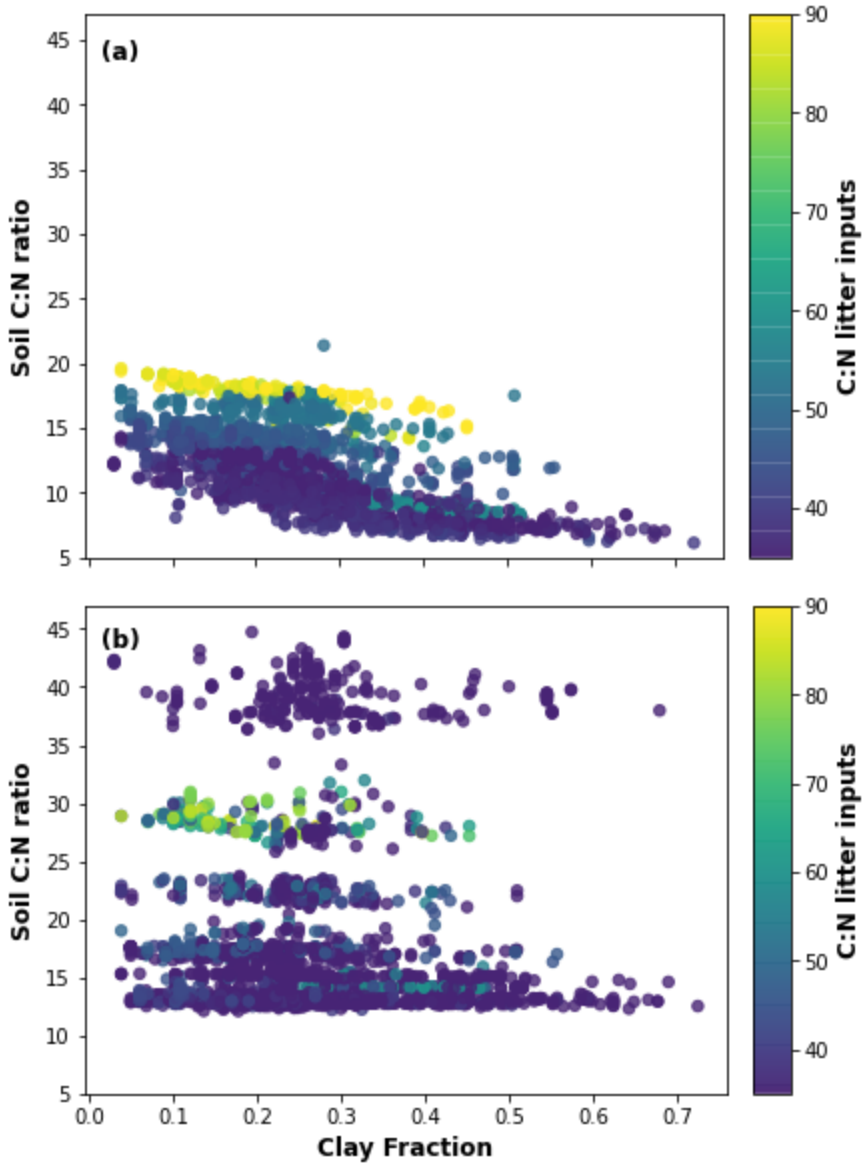


**Figure 5**. Soil texture and litter quality effects on soil C:N ratio that are simulated in (**a**) MIMICS-CN but not (**b**) CASA-CN. MIMICS assumes that clay content and litterfall chemistry interact to determine bulk soil C:N ratios. By contrast, CASA applies a biome-specific soil stoichiometric parameterization and does not reflect influences of soil texture or litter quality on soil C:N ratios. Coarse woody debris stoichiometry is considered in the litterfall C:N ratio in MIMICS-CN, but not in CASA-CN, which produces different litterfall stoichiometry estimates between the two models. The color bars used here match the one used in Fig 4c.

### 3.2. Transient response

Global GPP simulated by CLM5 increased from 106 Pg C $y^{-1}$ at the start of the 20th century to 125 Pg C $y^{-1}$ by the end of the historical period (here 2014). This led to an increase in NPP simulated by all the models, with the C-only models showing a slightly higher increase in NPP than the CN models (Table 2, Figs. 6a, S2). These increases in productivity and modest

climate warming drove accelerated rates of heterotrophic respiration and net N mineralization in both models (Fig. 6 c-d). On balance, CASA simulations show accumulations of soil organic C and a more robust land C sink than MIMICS simulations, which indicate soil C losses and weaker (or neutral) land C uptake over the historical period (Figs. 6 e-f; S2).

**Table 2**. Summary of the change in annual fluxes and states simulated by MIMICS and CASA models with CN and C-only biogeochemistry at the end of the historical period. Values represent global sums and means of annual data from 1995-2014 subtracted by those calculated at initialization in Table 1.

| **Δ in fluxes and states** | **MIMICS-CN** | **MIMICS C-only** | **CASA-CN** | **CASA C-only** |
|---|---|---|---|---|
| **GPP (Pg C $y^{-1}$)** | 15.5 | 15.5 | 15.5 | 15.5 |
| **NPP (Pg C $y^{-1}$)** | 5.5 | 5.6 | 5.5 | 5.6 |
| **HR (Pg C $y^{-1}$)** | 5.4 | 5.7 | 4.5 | 4.9 |
| **Total soil C (Pg C)** | -14 | -24 | 7 | 6 |
| **Total vegetation C (Pg C)** | 27 | 28 | 25 | 28 |
| **Microbial Biomass (Pg C)** | 1.2 | 1.2 | - | - |
| **Relative microbial biomass C (%)** | 0.1 | 0.1 | - | - |
| **Net N mineralization (Tg N $y^{-1}$)** | 119 | - | 107 | - |
| **Total soil C:N** | -0.07 | - | -0.03 | - |
| **Microbial C:N** | -0.03 | - | - | - |

At initialization, MIMICS-CN showed slightly stronger N-limitation of NPP than CASA-CN (Table 1; Fig. S1). Over the historical period, N limitation increased in both models, but more so in CASA-CN (Fig 6b). Greater vegetation C accumulation in MIMICS-CN, compared to CASA-CN (Table 2) was fueled by changes in soil biogeochemistry. Over the historical period, MIMICS-CN simulated larger increase in heterotrophic respiration and net N mineralization that resulted in soil C losses and a weak to neutral land C sink compared to CASA-CN, which accumulated soil C over this time and showed a stronger land C sink (Table 2; Figs. 6c-f, S2). Notably, MIMICS also simulated greater interannual variability in global C and N fluxes, compared to CASA simulations, despite receiving identical climate forcings (Fig. 6b-d).

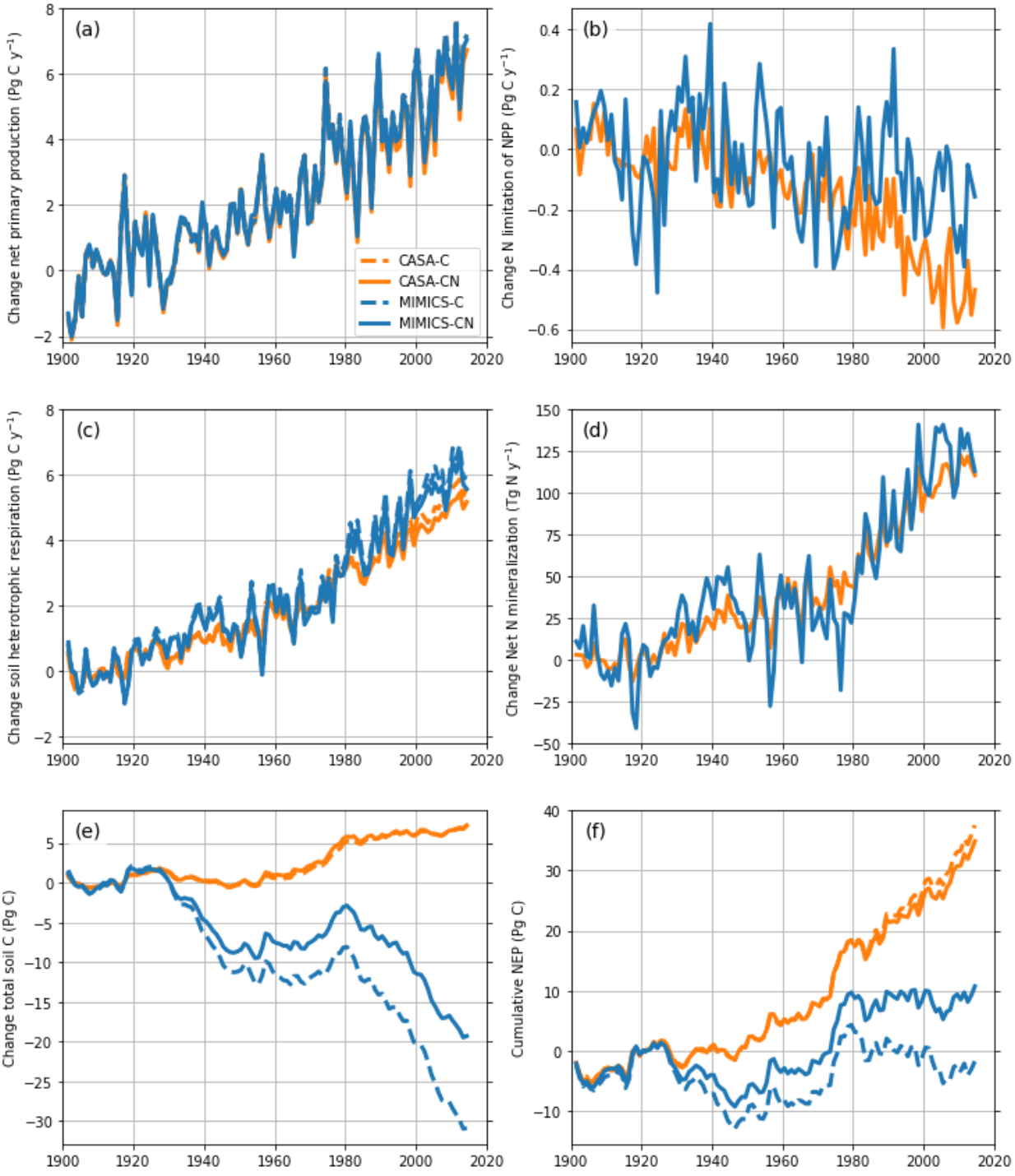
(a)
Change net primary production (Pg C y⁻¹)
CASA-C
CASA-CN
MIMICS-C
MIMICS-CN
(b)
Change N limitation of NPP (Pg C y⁻¹)
(c)
Change soil heterotrophic respiration (Pg C y⁻¹)
(d)
Change Net N mineralization (Tg N y⁻¹)
(e)
Change total soil C (Pg C)
(f)
Cumulative NEP (Pg C)

**Figure** 6. Change in global ecosystem stocks and fluxes simulated by MIMICS and CASA (blue and orange lines, respectively) with coupled CN biogeochemistry and C-only configuration (solid and dashed lines, respectively). Panels show changes in global (**a**) net primary production (NPP), (**b**) nitrogen limitation of NPP (difference of CN and C-only simulations), (**c**) heterotrophic respiration, (**d**) net nitrogen mineralization, (**e**) total soil C, and (**f**) cumulative net ecosystem production (NEP). In all plots, the change in annual values from the historical simulation are subtracted from the initial (1901-1920) global mean.

A closer look at regional dynamics helps illuminate differences in MIMICS vs. CASA simulations. Here we focus on the mean climatology of daily results simulated over a boreal forest region in Northern Europe (60-70°N & 0-100°E) at initialization (1901-1905 mean) and at the end of the historical period (2010-2014 mean). At steady state, MIMICS is more N limited than CASA (both globally and in this region; Figs. S1, Fig. 7). Over the historical period, however, MIMICS becomes less N limited, largely because of temperature driven increases in SOM turnover at high latitudes (Fig 7; Fig S2).

In our region of focus, mean NPP simulated during the model initialization period was 217 vs. 265 gC $m^{-2}$ $y^{-1}$ for MIMICS-CN and CASA-CN, respectively (Fig. 7a; dashed lines). Low soil inorganic N concentrations simulated by both models caused this N limitation (Fig. 7c, 7e). Collectively, these results illustrate differences in model sensitivities to cold soil temperatures that characterize the region. For most of the year, frozen soils more strongly limit microbial activity in MIMICS-CN, resulting in lower heterotrophic respiration and N mineralization fluxes in the boreal winter, spring, and fall, but higher rates during the warmer summer months (Fig. 7b, 7d, 7f). Notably, annual heterotrophic respiration fluxes are equal to NPP fluxes that are simulated by both models at initialization; therefore, initial NEP equals zero for both models, but differences in the environmental sensitivities of MIMICS and CASA results in distinct seasonal climatologies of the timing of these fluxes during the year.

By the end of the historical period, differences in annual productivity that are simulated by the two models are reduced (Fig. 7). Annual NPP totaled 291 vs. 313 gC $m^{-2}$ $y^{-1}$ in MIMICS-CN and CASA-CN, respectively; an increase of 34% and 18%, relative to their initial rates. Concurrently, in both models, warmer soil temperatures and higher productivity accelerate soil biogeochemical transformations. By the end of the historical period, annual heterotrophic rates increased by 30% and 14% in MIMICS-CN and CASA-CN, respectively, while net N mineralization rates increased by 39% and 20%, relative to their initial rates. This increases inorganic N availability, decreases the extent of N limitation, and fuels greater NPP. Although MIMICS-CN shows a stronger acceleration of NPP and HR fluxes over this domain, it still has dampened terrestrial C uptake (regional mean NEP = 9.1 and 10.0 gC $m^{-2}$ $y^{-1}$ in MIMICS-CN and CASA-CN, respectively). By comparison NEP fluxes over this domain for C-only models show much larger spread (regional mean NEP = -12.0 and 10.9 gC $m^{-2}$ $y^{-1}$ in the C only versions of MIMICS and CASA, respectively). Thus, inclusion of coupled CN biogeochemistry dampens the net carbon cycle response of both models over the historical period, relative to the C-only models, a result that is also evident in our global results (Fig. 6f).

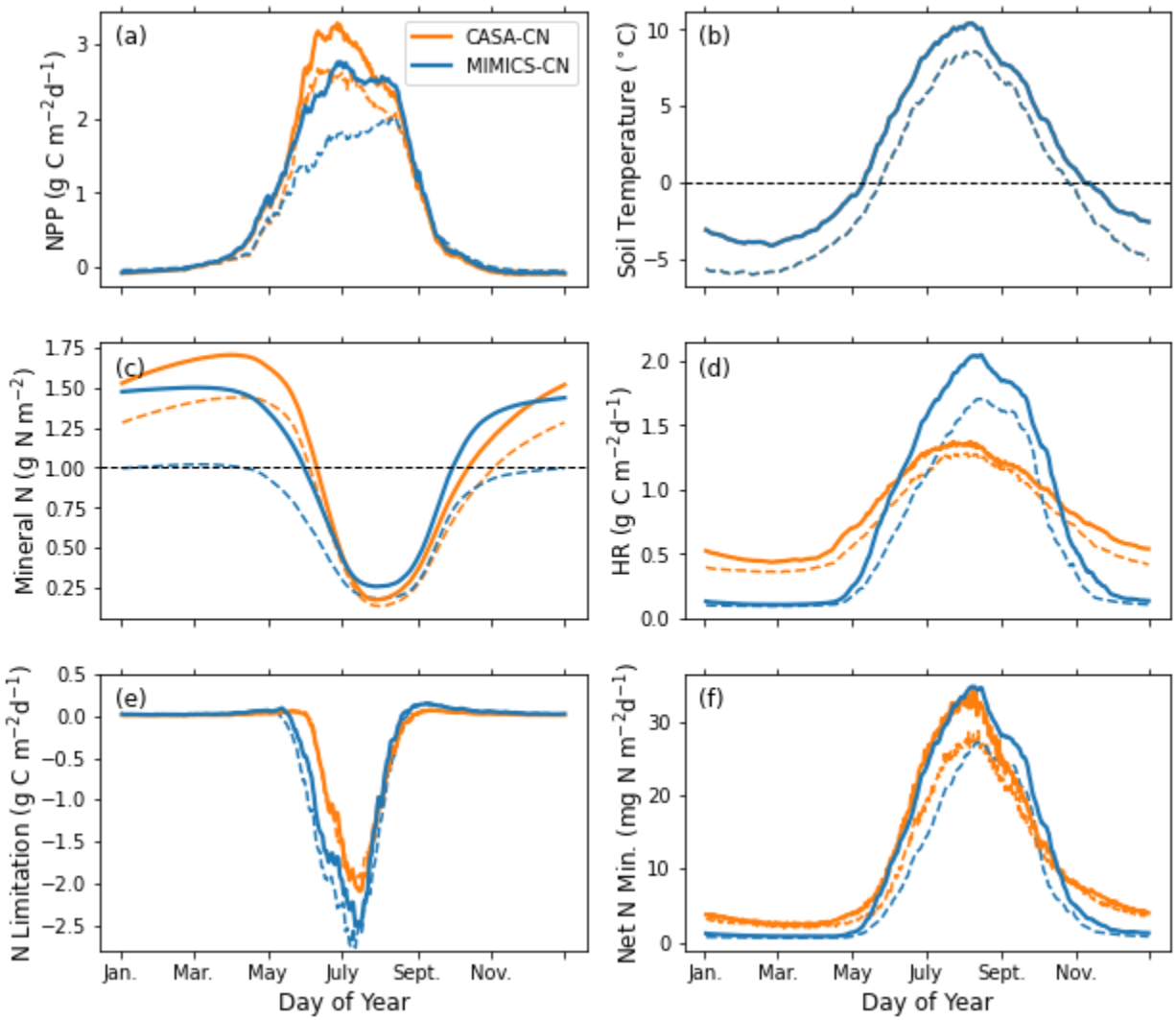


**Figure 7**. Mean annual cycle of ecosystem fluxes and states simulated by MIMICS and CASA (blue and orange lines, respectively) with coupled CN biogeochemistry at the start (1901-1905; dashed line) end of the historical simulation (2010-2014; solid lines) over Northern Europe (60-70 °N & 0-100 °E). Panels show the annual cycle in the regionally averaged (**a**) net primary production (NPP), (**b**) soil temperature, (0-50 cm) (**c**) mineral N stocks, (**d**) heterotrophic respiration, (**e**) N limitation of NPP, and (**f**) net N mineralization rates.

## 4 Discussion

With common boundary conditions, the addition of coupled CN biogeochemistry to the MIMICS and CASA soil biogeochemical models produces global-scale results that are largely comparable with their respective C-only versions (Table 1). Steady-state soil C pools and turnover times that are simulated by MIMICS and CASA still show notable differences in their global sums and latitudinal distribution (Figs. 2-3). Furthermore, simulation of coupled CN biogeochemistry dampens the C cycle response in transient simulations. Increasing N limitation in CASA-CN resulted in lower rates of vegetation C accrual over the historical period, compared

with the C-only simulations (Table 2, Fig. 6); a finding that is consistent with previous modeling studies (Thornton et al., 2007; Y. P. Wang et al., 2010; Zaehle et al., 2010). By contrast, vegetation C accrual in MIMICS-CN nearly matched the C-only version of the model (Table 2). This occurred because higher rates of N mineralization were fueled by warming-induced accelerations of SOM decomposition over high latitude ecosystems during the historical period (Figs. 6-7, S2 see also Wieder et al. 2018). Thus, simulating CN biogeochemistry attenuated high latitude soil C losses that were simulated by MIMICS over the historical period, which actually increased cumulative NEP, relative to the C-only version of this model.

Collectively, differences between MIMICS and CASA are larger than the effects of considering CN biogeochemistry in the respective models (see also Wieder et al., 2018; Wieder et al., 2019). Differences in model parameterizations and model structures are responsible for these findings, and should be explored in future research (Luo et al., 2016; Pierson et al., 2022; Shi et al., 2018; Ying-Ping Wang et al., 2021; H. Zhang et al., 2020). Instead, we emphasize some of the theoretical differences between explicit and implicit representations of microbial activity and their influence on emergent properties of the biogeochemical system. We first discuss how these results highlight differences in the underlying assumptions of MIMICS and CASA. Subsequently, we discuss the advantages and drawbacks of using SOM C:N stoichiometry as an emergent property in soil biogeochemical models. Finally, we explore implications and future directions for applying microbial explicit structures to explore coupled C-nutrient dynamics in land models.

### 4.1 Underlying model assumptions

The representation of CN biogeochemistry does not modify the steady-state turnover time of SOM pools that are represented by CASA, but it does in MIMICS (Fig. 2). Models that implicitly represent microbial activity assume that the turnover time of SOM pools are determined by the inherent biochemical quality of substrates and modified by environmental scalars (Luo et al., 2016; Joshua P. Schimel, 2001). Accordingly, CASA simulations show no change in the inferred soil C turnover times with coupled CN biogeochemistry. By contrast, models that explicitly represent microbial activity assume that SOM turnover times are influenced by the size and activity of microbial biomass pools. This has important implications for both steady-state soil C pools, as well as seasonal dynamics of heterotrophic respiration (Basile et al., 2020; Jian et al., 2021) and N mineralization fluxes in microbially-explicit models like MIMICS (Fig 7).

Microbial biomass pools in MIMICS both build and decay SOM. The size of microbial biomass pools simulated in the model are proportional to litterfall C inputs (Wieder, Grandy, et al., 2015). Nitrogen limitation of NPP reduces litterfall, which also reduces microbial biomass pools that are simulated by MIMICS-CN (Table 1; Fig. 3). Across all gridcells globally, the response of soil C turnover times in MIMICS-CN is negatively correlated with these changes in microbial biomass (Fig. 2c). Thus, N limitation of NPP in the MIMICS-CN simulations reduces microbial biomass C and microbial catabolic potential to decompose SOM. This results in longer soil C turnover times, relative to the C-only simulations in MIMICS-CN. We see the largest effects of N-limitation on NPP across high latitude ecosystems (Fig. S1), where N effects on SOM turnover times are also most pronounced (Fig. 2).

Explicitly representing microbial activity also influences temporal dynamics of soil biogeochemical fluxes that are simulated by MIMICS, and other microbial explicit models (Y. Huang et al., 2021). This is evident in the higher interannual variability of heterotrophic

respiration and N mineralization fluxes that are simulated by MIMICS-CN (Fig. 6). For example, regional biogeochemical fluxes that are simulated by MIMICS-CN show higher seasonal amplitude, a larger response to warming over the historical period, and a slight temporal lag in peak fluxes, relative to the CASA-CN simulations (Fig. 7). Previous work found similar patterns with C-only versions of these models (Wieder et al., 2018) that have important implications on global estimates of terrestrial net ecosystem exchange of $CO_2$ with the atmosphere (Basile et al., 2020). The differences simulated by MIMICS and CASA, therefore, present opportunities for future studies to consider how changes in microbial physiology and phenology may impact the temporal dynamics of N mineralization rates and their feedback to ecosystem C and N fluxes under climate change scenarios.

The mathematical representation of nutrient limitation in land models continues to be challenging (Kou-Giesbrecht et al., 2023; Thomas et al., 2015). We recognize that CASA-CNP applies a relatively simplistic approach to plant N limitation by downregulating NPP and heterotrophic respiration rates when inorganic N pools are small (< 1g N $m^{-2}$; Wang et al. 2010). Similar assumptions are made by other microbial implicit soil biogeochemical models, which calculate potential rates of soil biogeochemical fluxes that are downregulated by nutrient availability (Lawrence et al., 2019; Yang et al., 2019; Zhu et al., 2019). By contrast, potential rates of litter and SOM decomposition are not downregulated by inorganic N availability in MIMICS-CN (Kyker-Snowman et al., 2020). Instead, if N availability is inadequate to meet microbial stoichiometric demands, then microbes reduce their effective CUE through overflow respiration fluxes that essentially burn off the excess carbon being decomposed. Additionally, the target stoichiometry of microbial communities varies as a function of litter quality in MIMICS-CN. Thus, the relative abundance of microbial functional groups shifts as a function of litter quality, but so too do their target C:N ratios (Fig. 4; eq. 1). Although this approach still simplifies the diversity of strategies different decomposers use to meet stoichiometric imbalances between microbial communities and their resources (Mooshammer et al., 2014; Zechmeister-Boltenstern et al., 2015), the assumptions made in MIMICS-CN are more in line with concepts of microbial trait theory than those in CASA-CN.

In MIMICS, the size of the microbial biomass pool moderates SOM turnover times, and therefore N mineralization rates (Fig. 2c). Accordingly, the relative size of microbial biomass pools, as a fraction of total soil C stocks, is a useful, first-order benchmark by which to evaluate microbial explicit models (Fierer et al., 2009; Serna-Chavez et al., 2013; Xu et al., 2013). The parameterization of MIMICS simulates larger relative microbial biomass pools in wetter ecosystems that support higher NPP (tropical and temperate forests) and smaller relative microbial biomass pools in drier, lower productivity regions (Fig. 3c). This pattern aligns well with observational estimates synthesized by Serna-Chavez et al. (2013), who similarly found a correlation between moisture availability and relative microbial biomass C. We note that another synthesis (Xu et al., 2013) reports similar patterns, but also reports even higher relative microbial biomass C in deserts.

Beyond microbial biomass, cross-biome differences in microbial traits may ultimately be more valuable for informing and evaluating models that explicitly represent microbial activity. For example, plant trait variation across environmental gradients may be critical for representing biotic control (and variation) in terrestrial energy, water, and biogeochemical fluxes (Butler et al., 2017; Díaz et al., 2022). Similar information about environmental controls over soil microbial traits will be critical to further developing models that explicitly represent microbial activity. For example, cross-system syntheses suggest that the microbial strategies and

biogeochemical function in arid systems may be distinct from more mesic environments (Fierer et al., 2012). Historical climate legacies may influence the physiological response of microbial communities to environmental change (Bradford et al., 2021; Evans & Wallenstein, 2014; Hawkes et al., 2020; Polussa et al., 2021). Finally, the phenology of microbial activity may lead to distinct seasonal shifts in microbial community composition (Lipson & Schmidt, 2004). In summary, mounting evidence suggests that microbial physiological traits show ecologically important variability over space and time, but they remain coarsely represented in the global parameterization of MIMICS-CN presented here. Thus, we see opportunities to further refine the model structure and parameterizations to improve the representation of microbial community composition and activity.

### 4.2 Stoichiometry as an emergent property

The stoichiometry of SOM in MIMICS-CN is an emergent property of the model, presenting opportunities to investigate model assumptions that produce variations in microbial biomass and SOM stoichiometry across climate, ecosystem, and edaphic gradients. In MIMICS-CN we assume that the higher catabolic capacity of fast growing copiotrophic microbial communities require more N and, therefore, these communities have a lower microbial biomass C:N ratio than slower growing oligotrophic communities. We also assume that the chemical quality of litter inputs modifies microbial biomass C:N, similar to assumptions made about litter quality and SOM stoichiometry in CASA and the CENTURY model (Parton et al., 1993). This results in relatively constrained estimates of microbial biomass C:N by MIMICS-CN, consistent with findings from observational syntheses (Cleveland & Liptzin, 2007; Xu et al., 2013). The spatial variation in microbial stoichiometry that is simulated by MIMICS is consistent with observationally derived extrapolations across latitudes (Fig. 3f; Gao et al., 2022; Xu et al., 2013) and largely reflects differences in the relative abundance of fast and slow growing microbes and the chemical quality of litter inputs (Figs. 4, 5). Still, real ecosystems have larger variation in microbial stoichiometry than the MIMICS-CN simulations presented here (Kyker-Snowman et al., 2020), presenting opportunities to deepen understanding of the ecological factors that may mediate microbial community stoichiometry within and among ecosystems.

In MIMICS-CN we not only assume that microbial biomass pools determine rates of decomposition, but also the formation of persistent SOM (orange lines, Fig 1). Accordingly, the stoichiometry of SOM pools show a strong microbial signature, in line with current understanding of SOM formation (Fig. 4; Kyker-Snowman et al., 2020; Whalen et al., 2022). This results in somewhat narrower latitudinal gradients and spatial variation in SOM C:N than observationally derived estimates (Fig. 3e). Collectively, however, MIMICS-CN makes clear assumptions that litter quality and soil texture are dominant controls over bulk soil C:N ratios that are simulated across ecosystems (Fig. 5). Bulk soil C:N values more broadly reflect the relative abundance of physically vs. chemically protected SOM, as expected theoretically and shown in observational data (Buchkowski et al., 2019; Cotrufo et al., 2019). For example, we assume clay-rich soils have a higher proportion of total SOM stocks in physicochemically protected (MAOM-like) pools (Grandy & Neff, 2008; Wieder et al., 2014). In MIMICS-CN the $SOM_p$ pool has a low C:N ratio that reflects the dominant role of microbial residues in forming this persistent pool of SOM that has long turnover times. By contrast, in sandier soils MIMICS-CN assumes a higher proportion of total SOM stocks are in chemically protected (POM-like) pools. The $SOM_c$ pool has a higher C:N ratio that reflects greater contributions of plant residues. Relative to the C-only version of MIMICS, the parameterization used in MIMICS-CN assumes

that a greater fraction of structural litter inputs bypass the microbial filter to form $SOM_c$, which is similar to a particulate organic matter (POM) pool (see also Kyker-Snowman et al., 2020). This modification was needed to increase the total soil C:N that is simulated in MIMICS-CN, although we also recognize that the current parameterization may overestimate the size of the $SOM_c$ pool globally, and especially at high latitudes (Wieder et al., 2019).

Potential low bias in bulk soil C:N ratios that are simulated by MIMICS-CN also underscore challenges in understanding plant vs. microbial contributions to SOM formation (Simpson et al., 2007; Whalen et al., 2022). This is especially true for SOM that is protected by minerals and aggregates, which tend to have longer turnover times. In MIMICS-CN, we assume that plant-derived biomolecules have a higher C:N ratio than those that are microbial-derived (Cleveland & Liptzin, 2007; Mooshammer et al., 2014), reflecting stoichiometric differences that may be helpful in evaluating the underlying assumptions in the model. Notably, recent work finds that plant-derived biomolecules are abundant within protected SOM, especially in forested ecosystems (Angst et al., 2021). Elsewhere, Heckman et al. (2023) found that MAOM from humid, forest soils tends to have higher C:N ratios that is less decomposed than MAOM from drier, grassland ecosystems. Additionally, exo-enzyme transformation of plant inputs, as opposed to microbial turnover, may increase OM contribution to MAOM with a more plant-like signature (Liang et al., 2017). Collectively, these findings underscore broader uncertainties in quantifying plant vs. microbial contributions to SOM formation (Whalen et al., 2022), but they also suggest that the current parameterization of MIMICS-CN may overemphasize the importance of microbial biomass contributions to protected SOM, which may also explain some of the low biases in bulk soil C:N ratios in our results.

In contrast to the emergent stoichiometry that reflects underlying assumptions made in MIMICS-CN, spatial variation in soil stoichiometry simulated by CASA-CN is less nuanced (Fig. 5). In models that implicitly represent microbial activity (including CASA-CNP) receiver pool stoichiometry is parameterized, either with a fixed value for particular pools (e.g.; lower C:N targets for the passive pool, ~11-12, compared to the slow pool, C:N ~12-20), that may also vary plant functional type (Koven et al., 2013; Y. P. Wang et al., 2010). This PFT-specific parameterization of SOM stoichiometry results in latitudinal gradients of soil C:N ratios simulated by CASA-CN (Fig. 3e). Stoichiometric flexibility is achieved through a linear function between soil C:N ratios and soil mineral N availability, which reduces receiver pool demand for N when mineral N availability is low and buffers soil C turnover from becoming limited by inorganic N availability (Bonan et al., 2013; Meyerholt & Zaehle, 2015; Parton et al., 1993; Y. P. Wang et al., 2010). Warmer sites have higher N mineralization rates and (slightly) lower soil C:N ratios, but in general soil stoichiometry simulated by CASA-CN largely reflects the PFT-specific parameterization applied in the model. While this parameterization of stoichiometric flexibility reflects foundational understanding of N mineralization, it has recently been suggested that N mineralization may be limited by desorption of N-rich MAOM, which is not well represented in MIMICS-CN or CASA-CN (Jilling et al., 2018; Jilling et al., 2021; J. P. Schimel & Bennett, 2004).

### 4.3 Implications and future directions

Our results illustrate the feasibility of conducting global scale simulations with a microbial explicit soil biogeochemical model under climate change scenarios. In both MIMICS and CASA simulations the inclusion of CN biogeochemistry attenuates or dampens the magnitude of ecosystem C responses to climate change over the historical period. The explicit

representation of microbial activity in MIMICS-CN modifies steady-state and transient behavior of the model, relative to its C-only counterpart. For example, by reducing litterfall and microbial biomass C, representing CN biogeochemistry increases the steady-state turnover time of SOM that is simulated by MIMICS-CN. Moreover, whereas nutrient limitation typically slows down decomposition of SOM pools that are simulated by microbial implicit models, MIMICS does not share this assumption, allowing for overflow respiration of excess C instead. However, concentration alone may not predict nutrient availability and future model development could include plant and microbial competition and other mechanisms underlying nutrient availability.

Beyond this direct consideration of nutrient limitation, shifts in plant and microbial resource allocation in response to global change drivers are important to consider, but only rudimentarily represented in the biogeochemical model testbed. For example, elevated $CO_2$ and N enrichment can alter plant belowground allocation, fine root stoichiometry, and microbial community composition (Drigo et al., 2010; Jia et al., 2023; Knops et al., 2007). Recent evidence shows that belowground C inputs are more efficiently stabilized on mineral surfaces and in aggregates (Austin et al., 2017; Sokol & Bradford, 2018). At the same time, root exudates and organic acids can prime decomposition of existing SOM and even destabilize MAOM to accelerate heterotrophic respiration and ecosystem C losses (Keiluweit et al., 2015; van Groenigen et al., 2014). Thus, the net effects of changing belowground C inputs on the long term persistence of SOM, N mineralization rates, and feedbacks to NPP ultimately influence the magnitude and direction of net terrestrial exchange of $CO_2$ with the atmosphere. Current assumptions made in the biogeochemical model testbed do not easily allow consideration of these dynamics. Future research will refine understanding of plant-soil feedbacks and apply these insights in an ensemble of models that represent coupled CN biogeochemistry.

Finally, by allowing SOM stoichiometry to be an emergent property of the model, we see opportunities to use MIMICS-CN to deepen understanding of plant vs. microbial sources of persistent SOM (Whalen et al., 2022). MIMICS-CN could also be altered to test alternative controls of N mineralization, such as desorption from the N-rich MAOM pool (Jilling et al., 2018). Further, soil C:N is a valuable metric for understanding soil C storage, N availability, and the N requirement of C storage (Averill, 2014; Cotrufo et al., 2019). The emergent stoichiometry in MIMICS-CN will allow for exploration of potential sensitivities of soil C:N to environmental change across gradients in soil properties, ecosystems, and climate, which have been inconsistently documented in observational studies (Keller et al., 2022; Rocci et al., 2022; Yue et al., 2017). Overall, applying coupled CN biogeochemistry in a microbially explicit model at the global scale for the first time allowed us to evaluate the effect of including microbes explicitly and also N, rather than solely C, which provided insight for model parameterizations but also future avenues of exploration.

## Acknowledgments

The authors declare no real or perceived financial conflicts of interests. We also do not have other affiliations that may be perceived as having a conflict of interest with respect to the results of this paper. This material is based upon work supported by the National Center for Atmospheric Research, which is a major facility sponsored by the National Science Foundation (NSF).

## Open Research

Model code and scripts used to generate figures are available from Wieder et al. (2023). Data including meterological drivers and testbed output are available from Wieder and Hartman (2023).

## References


Angst, G., Mueller, K. E., Nierop, K. G. J., & Simpson, M. J. (2021). Plant- or microbial-derived? A review on the molecular composition of stabilized soil organic matter. *Soil Biology and Biochemistry, 156*, 108189. doi: 10.1016/j.soilbio.2021.108189.

Austin, E. E., Wickings, K., McDaniel, M. D., Robertson, G. P., & Grandy, A. S. (2017). Cover crop root contributions to soil carbon in a no-till corn bioenergy cropping system. *GCB Bioenergy, 9*(7), 1252-1263. doi: 10.1111/gcbb.12428.

Averill, C. (2014). Divergence in plant and microbial allocation strategies explains continental patterns in microbial allocation and biogeochemical fluxes. *Ecology Letters, 17*(10), 1202-1210. doi: 10.1111/ele.12324.

Averill, C., Turner, B. L., & Finzi, A. C. (2014). Mycorrhiza-mediated competition between plants and decomposers drives soil carbon storage. *Nature, 505*, 543. doi: 10.1038/nature12901.

Basile, S. J., Lin, X., Wieder, W. R., Hartman, M. D., & Keppel-Aleks, G. (2020). Leveraging the signature of heterotrophic respiration on atmospheric CO2 for model benchmarking. *Biogeosciences, 17*(5), 1293-1308. doi: 10.5194/bg-17-1293-2020.

Bonan, G. B., Hartman, M. D., Parton, W. J., & Wieder, W. R. (2013). Evaluating litter decomposition in earth system models with long-term litterbag experiments: an example using the Community Land Model version 4 (CLM4). *Global Change Biology, 19*, 957–974. doi: 10.1111/gcb.12031.

Bonan, G. B., Lombardozzi, D. L., Wieder, W. R., Oleson, K. W., Lawrence, D. M., Hoffman, F. M., & Collier, N. (2019). Model Structure and Climate Data Uncertainty in Historical Simulations of the Terrestrial Carbon Cycle (1850–2014). *Global Biogeochemical Cycles, 33*(10), 1310-1326. doi: 10.1029/2019gb006175.

Bradford, M. A., Wood, S. A., Addicott, E. T., Fenichel, E. P., Fields, N., González-Rivero, J., Jevon, F. V., Maynard, D. S., Oldfield, E. E., Polussa, A., Ward, E. B., & Wieder, W. R. (2021). Quantifying microbial control of soil organic matter dynamics at macrosystem scales. *Biogeochemistry, 156*(1), 19-40. doi: 10.1007/s10533-021-00789-5.

Buchkowski, R. W., Shaw, A. N., Sihi, D., Smith, G. R., & Keiser, A. D. (2019). Constraining Carbon and Nutrient Flows in Soil With Ecological Stoichiometry. *Frontiers in Ecology and Evolution, 7*. doi: 10.3389/fevo.2019.00382.

Butler, E. E., Datta, A., Flores-Moreno, H., Chen, M., Wythers, K. R., Fazayeli, F., Banerjee, A., Atkin, O. K., Kattge, J., Amiaud, B., Blonder, B., Boenisch, G., Bond-Lamberty, B., Brown, K. A., Byun, C., Campetella, G., Cerabolini, B. E. L., Cornelissen, J. H. C., Craine, J. M., Craven, D., de Vries, F. T., Diaz, S., Domingues, T. F., Forey, E., Gonzalez-Melo, A., Gross, N., Han, W., Hattingh, W. N., Hickler, T., Jansen, S., Kramer, K., Kraft, N. J. B., Kurokawa, H., Laughlin, D. C., Meir, P., Minden, V., Niinemets, U., Onoda, Y., Penuelas, J., Read, Q., Sack, L., Schamp, B., Soudzilovskaia, N. A., Spasojevic, M. J., Sosinski, E., Thornton, P. E., Valladares, F., van Bodegom, P. M., Williams, M., Wirth, C., & Reich, P. B. (2017). Mapping local and global variability in plant trait distributions. *Proc Natl Acad Sci U S A, 114*(51), E10937-E10946. doi: 10.1073/pnas.1708984114.

Cleveland, C. C., & Liptzin, D. (2007). C:N:P stoichiometry in soil: is there a “Redfield ratio” for the microbial biomass? *Biogeochemistry, 85*(3), 235-252. doi: 10.1007/s10533-007-9132-0.

Cotrufo, M. F., Ranalli, M. G., Haddix, M. L., Six, J., & Lugato, E. (2019). Soil carbon storage informed by particulate and mineral-associated organic matter. *Nature Geoscience, 12*(12), 989-994. doi: 10.1038/s41561-019-0484-6.

Cotrufo, M. F., Wallenstein, M. D., Boot, C. M., Denef, K., & Paul, E. (2013). The Microbial Efficiency-Matrix Stabilization (MEMS) framework integrates plant litter decomposition with soil organic matter stabilization: do labile plant inputs form stable soil organic matter? *Global Change Biology, 19*(4), 988-995. doi: 10.1111/gcb.12113.

Díaz, S., Kattge, J., Cornelissen, J. H. C., Wright, I. J., Lavorel, S., Dray, S., Reu, B., Kleyer, M., Wirth, C., Prentice, I. C., Garnier, E., Bönisch, G., Westoby, M., Poorter, H., Reich, P. B., Moles, A. T., Dickie, J., Zanne, A. E., Chave, J., Wright, S. J., Sheremetiev, S. N., Jactel, H., Baraloto, C., Cerabolini, B. E. L., Pierce, S., Shipley, B., Casanoves, F., Joswig, J. S., Günther, A., Falczuk, V., Rüger, N., Mahecha, M. D., Gorné, L. D., Amiaud, B., Atkin, O. K., Bahn, M., Baldocchi, D., Beckmann, M., Blonder, B., Bond, W., Bond-Lamberty, B., Brown, K., Burrascano, S., Byun, C., Campetella, G., Cavender-Bares, J., Chapin, F. S., Choat, B., Coomes, D. A., Cornwell, W. K., Craine, J., Craven, D., Dainese, M., de Araujo, A. C., de Vries, F. T., Domingues, T. F., Enquist, B. J., Fagúndez, J., Fang, J., Fernández-Méndez, F., Fernandez-Piedade, M. T., Ford, H., Forey, E., Freschet, G. T., Gachet, S., Gallagher, R., Green, W., Guerin, G. R., Gutiérrez, A. G., Harrison, S. P., Hattingh, W. N., He, T., Hickler, T., Higgins, S. I., Higuchi, P., Ilic, J., Jackson, R. B., Jalili, A., Jansen, S., Koike, F., König, C., Kraft, N., Kramer, K., Kreft, H., Kühn, I., Kurokawa, H., Lamb, E. G., Laughlin, D. C., Leishman, M., Lewis, S., Louault, F., Malhado, A. C. M., Manning, P., Meir, P., Mencuccini, M., Messier, J., Miller, R., Minden, V., Molofsky, J., Montgomery, R., Montserrat-Martí, G., Moretti, M., Müller, S., Niinemets, Ü., Ogaya, R., Öllerer, K., Onipchenko, V., Onoda, Y., Ozinga, W. A., Pausas, J. G., Peco, B., Penuelas, J., Pillar, V. D., Pladevall, C., Römermann, C., Sack, L., Salinas, N., Sandel, B., Sardans, J., Schamp, B., Scherer-Lorenzen, M., Schulze, E.-D., Schweingruber, F., Shiodera, S., Sosinski, Ê., Soudzilovskaia, N., Spasojevic, M. J., Swaine, E., Swenson, N., Tautenhahn, S., Thompson, K., Totte, A., Urrutia-Jalabert, R., Valladares, F., van Bodegom, P., Vasseur, F., Verheyen, K., Vile, D., Violle, C., von Holle, B., Weigelt, P., Weiher, E., Wiemann, M. C., Williams, M., Wright, J., & Zotz, G. (2022). The global spectrum of plant form and function: enhanced species-level trait dataset. *Scientific Data*, *9*(1), 755. doi: 10.1038/s41597-022-01774-9.

Drigo, B., Pijl, A. S., Duyts, H., Kielak, A. M., Gamper, H. A., Houtekamer, M. J., Boschker, H. T., Bodelier, P. L., Whiteley, A. S., van Veen, J. A., & Kowalchuk, G. A. (2010). Shifting carbon flow from roots into associated microbial communities in response to elevated atmospheric CO2. *Proc Natl Acad Sci U S A*, *107*(24), 10938-10942. doi: 10.1073/pnas.0912421107.

Dunne, J. P., Horowitz, L. W., Adcroft, A. J., Ginoux, P., Held, I. M., John, J. G., Krasting, J. P., Malyshev, S., Naik, V., Paulot, F., Shevliakova, E., Stock, C. A., Zadeh, N., Balaji, V., Blanton, C., Dunne, K. A., Dupuis, C., Durachta, J., Dussin, R., Gauthier, P. P. G., Griffies, S. M., Guo, H., Hallberg, R. W., Harrison, M., He, J., Hurlin, W., McHugh, C., Menzel, R., Milly, P. C. D., Nikonov, S., Paynter, D. J., Ploshay, J., Radhakrishnan, A., Rand, K., Reichl, B. G., Robinson, T., Schwarzkopf, D. M., Sentman, L. T., Underwood, S., Vahlenkamp, H., Winton, M., Wittenberg, A. T., Wyman, B., Zeng, Y., & Zhao, M. (2020). The GFDL Earth System Model Version 4.1 (GFDL-ESM 4.1): Overall Coupled Model Description and Simulation Characteristics. *Journal of Advances in Modeling Earth Systems*, *12*(11), e2019MS002015. doi: 10.1029/2019ms002015.

Eastman, B. A., Wieder, W. R., Hartman, M. D., Brzostek, E. R., & Peterjohn, W. T. (2023). Can models adequately reflect how long-term nitrogen enrichment alters the forest soil carbon cycle? *Biogeosciences Discuss.*, *2023*, 1-33. doi: 10.5194/bg-2023-36.

Elser, J. J., Bracken, M. E. S., Cleland, E. E., Gruner, D. S., Harpole, W. S., Hillebrand, H., Ngai, J. T., Seabloom, E. W., Shurin, J. B., & Smith, J. E. (2007). Global analysis of nitrogen and phosphorus limitation of primary producers in freshwater, marine and terrestrial ecosystems. *Ecology Letters*, *10*(12), 1135-1142. doi:

Evans, S. E., & Wallenstein, M. D. (2014). Climate change alters ecological strategies of soil bacteria. *Ecol Lett*, *17*(2), 155-164. doi: 10.1111/ele.12206.

Fanin, N., Fromin, N., Buatois, B., & Hattenschwiler, S. (2013). An experimental test of the hypothesis of non-homeostatic consumer stoichiometry in a plant litter-microbe system. *Ecol Lett*, *16*(6), 764-772. doi: 10.1111/ele.12108.

Fanin, N., Hättenschwiler, S., & Fromin, N. (2014). Litter fingerprint on microbial biomass, activity, and community structure in the underlying soil. *Plant and Soil*, *379*(1-2), 79-91. doi: 10.1007/s11104-014-2051-7.

FAO, IIASA, ISRIC, ISSCAS, & JRC. (2012). *Harmonized World Soil Database (version 1.2)*. Retrieved from: http://webarchive.iiasa.ac.at/Research/LUC/External-World-soil-database/HTML/index.html?sb=1. doi: .

Fierer, N., Leff, J. W., Adams, B. J., Nielsen, U. N., Bates, S. T., Lauber, C. L., Owens, S., Gilbert, J. A., Wall, D. H., & Caporaso, J. G. (2012). Cross-biome metagenomic analyses of soil microbial communities and their functional attributes. *Proceedings of the National Academy of Sciences*, *109*(52), 21390-21395. doi: 10.1073/pnas.1215210110.

Fierer, N., Strickland, M. S., Liptzin, D., Bradford, M. A., & Cleveland, C. C. (2009). Global patterns in belowground communities. *Ecol Lett, 12*(11), 1238-1249. doi: 10.1111/j.1461-0248.2009.01360.x.

Gao, D., Bai, E., Wang, S., Zong, S., Liu, Z., Fan, X., Zhao, C., & Hagedorn, F. (2022). Three-dimensional mapping of carbon, nitrogen, and phosphorus in soil microbial biomass and their stoichiometry at the global scale. *Glob Chang Biol, 28*(22), 6728-6740. doi: 10.1111/gcb.16374.

Grandy, A. S., & Neff, J. C. (2008). Molecular C dynamics downstream: The biochemical decomposition sequence and its impact on soil organic matter structure and function. *Science of The Total Environment, 404*(2-3), 297-307. doi: 10.1016/j.scitotenv.2007.11.013.

Hashimoto, S., Carvalhais, N., Ito, A., Migliavacca, M., Nishina, K., & Reichstein, M. (2015). Global spatiotemporal distribution of soil respiration modeled using a global database. *Biogeosciences, 12*(13), 4121-4132. doi: 10.5194/bg-12-4121-2015.

Hawkes, C. V., Shinada, M., & Kivlin, S. N. (2020). Historical climate legacies on soil respiration persist despite extreme changes in rainfall. *Soil Biology and Biochemistry, 143*, 107752. doi: 10.1016/j.soilbio.2020.107752.

Heckman, K. A., Possinger, A. R., Badgley, B. D., Bowman, M. M., Gallo, A. C., Hatten, J. A., Nave, L. E., SanClements, M. D., Swanston, C. W., Weiglein, T. L., Wieder, W. R., & Strahm, B. D. (2023). Moisture-driven divergence in mineral-associated soil carbon persistence. *Proceedings of the National Academy of Sciences, 120*(7), e2210044120. doi: doi:10.1073/pnas.2210044120.

Huang, Y., Guenet, B., Ciais, P., Janssens, I. A., Soong, J. L., Wang, Y., Goll, D., Blagodatskaya, E., & Huang, Y. (2018). ORCHIMIC (v1.0), a microbe-mediated model for soil organic matter decomposition. *Geoscientific Model Development, 11*(6), 2111-2138. doi: 10.5194/gmd-11-2111-2018.

Huang, Y., Guenet, B., Wang, Y. L., & Ciais, P. (2021). Global Simulation and Evaluation of Soil Organic Matter and Microbial Carbon and Nitrogen Stocks Using the Microbial Decomposition Model ORCHIMIC v2.0. *Global Biogeochemical Cycles, 35*(5), e2020GB006836. doi: 10.1029/2020gb006836.

Hugelius, G., Tarnocai, C., Broll, G., Canadell, J. G., Kuhry, P., & Swanson, D. K. (2013). The Northern Circumpolar Soil Carbon Database: spatially distributed datasets of soil coverage and soil carbon storage in the northern permafrost regions. *Earth Syst. Sci. Data, 5*(1), 3-13. doi: 10.5194/essd-5-3-2013.

Jia, W., Zheng, T., Zhao, Y., Deng, F., Yang, Y., Liang, C., He, H., & Zhang, X. (2023). Nitrogen application influences the effect of bacteria on the belowground allocation of photosynthesized carbon under elevated CO2. *Soil Biology and Biochemistry, 180*, 109021. doi: 10.1016/j.soilbio.2023.109021.

Jian, J., Bond-Lamberty, B., Hao, D., Sulman, B. N., Patel, K. F., Zheng, J., Dorheim, K., Pennington, S. C., Hartman, M. D., Warner, D., & Wieder, W. R. (2021). Leveraging observed soil heterotrophic respiration fluxes as a novel constraint on global-scale models. *Glob Chang Biol, 27*(20), 5392-5403. doi: 10.1111/gcb.15795.

Jilling, A., Keiluweit, M., Contosta, A. R., Frey, S., Schimel, J., Schnecker, J., Smith, R. G., Tiemann, L., & Grandy, A. S. (2018). Minerals in the rhizosphere: overlooked mediators of soil nitrogen availability to plants and microbes. *Biogeochemistry, 139*(2), 103-122. doi: 10.1007/s10533-018-0459-5.

Jilling, A., Keiluweit, M., Gutknecht, J. L. M., & Grandy, A. S. (2021). Priming mechanisms providing plants and microbes access to mineral-associated organic matter. *Soil Biology and Biochemistry, 158*, 108265. doi: 10.1016/j.soilbio.2021.108265.

Keiluweit, M., Bougoure, J. J., Nico, P. S., Pett-Ridge, J., Weber, P. K., & Kleber, M. (2015). Mineral protection of soil carbon counteracted by root exudates. *Nature Climate Change, 5*(6), 588-595. doi: 10.1038/nclimate2580.

Keller, A. B., Borer, E. T., Collins, S. L., DeLancey, L. C., Fay, P. A., Hofmockel, K. S., Leakey, A. D. B., Mayes, M. A., Seabloom, E. W., Walter, C. A., Wang, Y., Zhao, Q., & Hobbie, S. E. (2022). Soil carbon stocks in temperate grasslands differ strongly across sites but are insensitive to decade-long fertilization. *Glob Chang Biol, 28*(4), 1659-1677. doi: 10.1111/gcb.15988.

Knops, J. M. H., Naeem, S., & Reich, P. B. (2007). The impact of elevated CO2, increased nitrogen availability and biodiversity on plant tissue quality and decomposition. *Global Change Biology, 13*(9), 1960-1971. doi: 10.1111/j.1365-2486.2007.01405.x.

Kou-Giesbrecht, S., Arora, V. K., Seiler, C., Arneth, A., Falk, S., Jain, A. K., Joos, F., Kennedy, D., Knauer, J., Sitch, S., O'Sullivan, M., Pan, N., Sun, Q., Tian, H., Vuichard, N., & Zaehle, S. (2023). Evaluating nitrogen cycling in terrestrial biosphere models: a disconnect between the carbon and nitrogen cycles. *Earth Syst. Dynam., 14*(4), 767-795. doi: 10.5194/esd-14-767-2023.

879 Koven, C. D., Hugelius, G., Lawrence, D. M., & Wieder, W. R. (2017). Higher climatological temperature
880 sensitivity of soil carbon in cold than warm climates. *Nature Climate Change, 7*(11), 817-822. doi:
881 10.1038/nclimate3421.
882 Koven, C. D., Riley, W. J., Subin, Z. M., Tang, J. Y., Torn, M. S., Collins, W. D., Bonan, G. B., Lawrence, D. M.,
883 & Swenson, S. C. (2013). The effect of vertically-resolved soil biogeochemistry and alternate soil C and N
884 models on C dynamics of CLM4. *Biogeosciences, 10*, 7109-7131. doi: 10.5194/bg-10-7109-2013.
885 Kyker-Snowman, E., Wieder, W. R., Frey, S. D., & Grandy, A. S. (2020). Stoichiometrically coupled carbon and
886 nitrogen cycling in the MIcrobial-MIneral Carbon Stabilization model version 1.0 (MIMICS-CN v1.0).
887 *Geoscientific Model Development, 13*(9), 4413-4434. doi: 10.5194/gmd-13-4413-2020.
888 Lawrence, D. M., Fisher, R. A., Koven, C. D., Oleson, K. W., Swenson, S. C., Bonan, G., Collier, N., Ghimire, B.,
889 Kampenhout, L., Kennedy, D., Kluzek, E., Lawrence, P. J., Li, F., Li, H., Lombardozzi, D., Riley, W. J.,
890 Sacks, W. J., Shi, M., Vertenstein, M., Wieder, W. R., Xu, C., Ali, A. A., Badger, A. M., Bisht, G., Broeke,
891 M., Brunke, M. A., Burns, S. P., Buzan, J., Clark, M., Craig, A., Dahlin, K., Drewniak, B., Fisher, J. B.,
892 Flanner, M., Fox, A. M., Gentine, P., Hoffman, F., Keppel-Aleks, G., Knox, R., Kumar, S., Lenaerts, J.,
893 Leung, L. R., Lipscomb, W. H., Lu, Y., Pandey, A., Pelletier, J. D., Perket, J., Randerson, J. T., Ricciuto,
894 D. M., Sanderson, B. M., Slater, A., Subin, Z. M., Tang, J., Thomas, R. Q., Val Martin, M., & Zeng, X.
895 (2019). The Community Land Model Version 5: Description of New Features, Benchmarking, and Impact
896 of Forcing Uncertainty. *Journal of Advances in Modeling Earth Systems, 11*(12), 4245-4287. doi:
897 10.1029/2018ms001583.
898 LeBauer, D. S., & Treseder, K. K. (2008). Nitrogen limitation of net primary productivity in terrestrial ecosystems is
899 globally distributed. *Ecology, 89*(2), 371-379. doi: 10.1890/06-2057.1.
900 Lehmann, J., Hansel, C. M., Kaiser, C., Kleber, M., Maher, K., Manzoni, S., Nunan, N., Reichstein, M., Schimel, J.
901 P., Torn, M. S., Wieder, W. R., & Kögel-Knabner, I. (2020). Persistence of soil organic carbon caused by
902 functional complexity. *Nature Geoscience, 13*(8), 529-534. doi: 10.1038/s41561-020-0612-3.
903 Lehmann, J., & Kleber, M. (2015). The contentious nature of soil organic matter. *Nature, 528*(7580), 60-68. doi:
904 10.1038/nature16069.
905 Li, Z., Tian, D., Wang, B., Wang, J., Wang, S., Chen, H. Y. H., Xu, X., Wang, C., He, N., & Niu, S. (2019).
906 Microbes drive global soil nitrogen mineralization and availability. *Glob Chang Biol, 25*(3), 1078-1088.
907 doi: 10.1111/gcb.14557.
908 Liang, C., Schimel, J. P., & Jastrow, J. D. (2017). The importance of anabolism in microbial control over soil carbon
909 storage. *Nat Microbiol, 2*, 17105. doi: 10.1038/nmicrobiol.2017.105.
910 Lipson, D. A., & Schmidt, S. K. (2004). Seasonal changes in an alpine soil bacterial community in the colorado
911 rocky mountains. *Appl Environ Microbiol, 70*(5), 2867-2879. doi: 10.1128/AEM.70.5.2867-2879.2004.
912 Luo, Y. Q., Ahlstrom, A., Allison, S. D., Batjes, N. H., Brovkin, V., Carvalhais, N., Chappell, A., Ciais, P.,
913 Davidson, E. A., Finzi, A. C., Georgiou, K., Guenet, B., Hararuk, O., Harden, J. W., He, Y. J., Hopkins, F.,
914 Jiang, L. F., Koven, C., Jackson, R. B., Jones, C. D., Lara, M. J., Liang, J. Y., McGuire, A. D., Parton, W.,
915 Peng, C. H., Randerson, J. T., Salazar, A., Sierra, C. A., Smith, M. J., Tian, H. Q., Todd-Brown, K. E. O.,
916 Torn, M., van Groenigen, K. J., Wang, Y. P., West, T. O., Wei, Y. X., Wieder, W. R., Xia, J. Y., Xu, X.,
917 Xu, X. F., & Zhou, T. (2016). Toward more realistic projections of soil carbon dynamics by Earth system
918 models. *Global Biogeochemical Cycles, 30*(1), 40-56. doi: 10.1002/2015gb005239.
919 Meyerholt, J., & Zaehle, S. (2015). The role of stoichiometric flexibility in modelling forest ecosystem responses to
920 nitrogen fertilization. *The New phytologist, 208*(4), 1042-1055. doi: 10.1111/nph.13547.
921 Mooshammer, M., Wanek, W., Zechmeister-Boltenstern, S., & Richter, A. (2014). Stoichiometric imbalances
922 between terrestrial decomposer communities and their resources: mechanisms and implications of
923 microbial adaptations to their resources. *Front Microbiol, 5*, 22. doi: 10.3389/fmicb.2014.00022.
924 Nemergut, D. R., Cleveland, C. C., Wieder, W. R., Washenberger, C. L., & Townsend, A. R. (2010). Plot-scale
925 manipulations of organic matter inputs to soils correlate with shifts in microbial community composition in
926 a lowland tropical rain forest. *Soil Biology & Biochemistry, 42*(12), 2153-2160. doi:
927 10.1016/j.soilbio.2010.08.011.
928 Parton, W. J., Schimel, D. S., Cole, C. V., & Ojima, D. S. (1987). Analysis of factors controlling soil organic-matter
929 levels in Great-Plains grasslands. *Soil Science Society Of America Journal, 51*(5), 1173-1179. doi:
930 10.2136/sssaj1987.03615995005100050015x
931 Parton, W. J., Scurlock, J. M. O., Ojima, D. S., Gilmanov, T. G., Scholes, R. J., Schimel, D. S., Kirchner, T.,
932 Menaut, J. C., Seastedt, T., Moya, E. G., Kamnalrut, A., & Kinyamario, J. I. (1993). Observations and
933 modeling of biomass and soil organic matter dynamics for the grassland biome worldwide. *Global*
934 *Biogeochemical Cycles, 7*(4), 785-809. doi: 10.1029/93GB02042.

Pierson, D., Lohse, K. A., Wieder, W. R., Patton, N. R., Facer, J., de Graaff, M.-A., Georgiou, K., Seyfried, M. S., Flerchinger, G., & Will, R. (2022). Optimizing process-based models to predict current and future soil organic carbon stocks at high-resolution. *Scientific Reports, 12*(1), 10824. doi: 10.1038/s41598-022-14224-8.

Poggio, L., de Sousa, L. M., Batjes, N. H., Heuvelink, G. B. M., Kempen, B., Ribeiro, E., & Rossiter, D. (2021). SoilGrids 2.0: producing soil information for the globe with quantified spatial uncertainty. *SOIL, 7*(1), 217-240. doi: 10.5194/soil-7-217-2021.

Polussa, A., Gonzalez-Rivero, J., Fields, N., Jevon, F. V., Wood, S. A., Wieder, W. R., & Bradford, M. A. (2021). Scale dependence in functional equivalence and difference in the soil microbiome. *Soil Biology and Biochemistry, 163*, 108451. doi: 10.1016/j.soilbio.2021.108451.

Rocci, K. S., Barker, K. S., Seabloom, E. W., Borer, E. T., Hobbie, S. E., Bakker, J. D., MacDougall, A. S., McCulley, R. L., Moore, J. L., Raynaud, X., Stevens, C. J., & Cotrufo, M. F. (2022). Impacts of nutrient addition on soil carbon and nitrogen stoichiometry and stability in globally-distributed grasslands. *Biogeochemistry, 159*(3), 353-370. doi: 10.1007/s10533-022-00932-w.

Schimel, J. P. (2001). 1.13-Biogeochemical Models: Implicit versus Explicit Microbiology. . In M. H. Ernst-Detlef Schulze, Sandy Harrison, Elisabeth Holland, Jonathan Lloyd, Ian Colin Prentice, David S. Schimel (Ed.), *Global Biogeochemical Cycles in the Climate System* (pp. 177–183): Academic Press.

Schimel, J. P., & Bennett, J. (2004). Nitrogen mineralization: Challenges of a changing paradigm. *Ecology, 85*, 591-602. doi:

Schimel, J. P., & Schaeffer, S. M. (2012). Microbial control over carbon cycling in soil. *Front Microbiol, 3*, 348. doi: 10.3389/fmicb.2012.00348.

Serna-Chavez, H. M., Fierer, N., & van Bodegom, P. M. (2013). Global drivers and patterns of microbial abundance in soil. *Global Ecology and Biogeography, 22*(10), 1162–1172. doi: 10.1111/geb.12070.

Shangguan, W., Dai, Y., Duan, Q., Liu, B., & Yuan, H. (2014). A global soil data set for earth system modeling. *Journal of Advances in Modeling Earth Systems, 6*(1), 249-263. doi: 10.1002/2013ms000293.

Shi, Z., Crowell, S., Luo, Y., & Moore, B. (2018). Model structures amplify uncertainty in predicted soil carbon responses to climate change. *Nature Communications, 9*(1), 2171. doi: 10.1038/s41467-018-04526-9.

Simpson, A. J., Simpson, M. J., Smith, E., & Kelleher, B. P. (2007). Microbially derived inputs to soil organic matter: are current estimates too low? *Environ Sci Technol, 41*(23), 8070-8076. doi: 10.1021/es071217x.

Sokol, N. W., & Bradford, M. A. (2018). Microbial formation of stable soil carbon is more efficient from belowground than aboveground input. *Nature Geoscience, 12*(1), 46-53. doi: 10.1038/s41561-018-0258-6.

Soong, J. L., Fuchslueger, L., Maranon-Jimenez, S., Torn, M. S., Janssens, I. A., Penuelas, J., & Richter, A. (2020). Microbial carbon limitation: The need for integrating microorganisms into our understanding of ecosystem carbon cycling. *Glob Chang Biol, 26*(4), 1953-1961. doi: 10.1111/gcb.14962.

Sulman, B. N., Phillips, R. P., Oishi, A. C., Shevliakova, E., & Pacala, S. W. (2014). Microbe-driven turnover offsets mineral-mediated storage of soil carbon under elevated $CO_2$. *Nature Climate Change, 4*(12), 1099-1102. doi: 10.1038/nclimate2436.

Sulman, B. N., Shevliakova, E., Brzostek, E. R., Kivlin, S. N., Malyshev, S., Menge, D. N. L., & Zhang, X. (2019). Diverse Mycorrhizal Associations Enhance Terrestrial C Storage in a Global Model. *Global Biogeochemical Cycles, 33*(4), 501-523. doi: 10.1029/2018gb005973.

Thomas, R. Q., Brookshire, E. N., & Gerber, S. (2015). Nitrogen limitation on land: how can it occur in Earth system models? *Glob Chang Biol, 21*(5), 1777-1793. doi: 10.1111/gcb.12813.

Thornton, P. E., Lamarque, J.-F., Rosenbloom, N. A., & Mahowald, N. M. (2007). Influence of carbon-nitrogen cycle coupling on land model response to CO2 fertilization and climate variability. *Global Biogeochemical Cycles, 21*(4), GB4018. doi: 10.1029/2006gb002868.

Thum, T., Caldararu, S., Engel, J., Kern, M., Pallandt, M., Schnur, R., Yu, L., & Zaehle, S. (2019). A new model of the coupled carbon, nitrogen, and phosphorus cycles in the terrestrial biosphere (QUINCY v1.0; revision 1996). *Geoscientific Model Development, 12*(11), 4781-4802. doi: 10.5194/gmd-12-4781-2019.

Todd-Brown, K. E. O., Randerson, J. T., Post, W. M., Hoffman, F. M., Tarnocai, C., Schuur, E. A. G., & Allison, S. D. (2013). Causes of variation in soil carbon predictions from CMIP5 Earth system models and comparison with observations. *Biogeosciences, 10*, 1717-1736. doi: 10.5194/bg-10-1717-2013.

van Groenigen, K. J., Qi, X., Osenberg, C. W., Luo, Y., & Hungate, B. A. (2014). Faster decomposition under increased atmospheric CO(2) limits soil carbon storage. *Science, 344*(6183), 508-509. doi: 10.1126/science.1249534.

Wang, G., Huang, W., Zhou, G., Mayes, M. A., & Zhou, J. (2020). Modeling the processes of soil moisture in regulating microbial and carbon-nitrogen cycling. *Journal of Hydrology, 585*, 124777. doi: 10.1016/j.jhydrol.2020.124777.

Wang, Y. P., Law, R. M., & Pak, B. (2010). A global model of carbon, nitrogen and phosphorus cycles for the terrestrial biosphere. *Biogeosciences, 7*(7), 2261-2282. doi: 10.5194/bg-7-2261-2010.

Wang, Y. P., Zhang, H., Ciais, P., Goll, D., Huang, Y., Wood, J. D., Ollinger, S. V., Tang, X., & Prescher, A. K. (2021). Microbial Activity and Root Carbon Inputs Are More Important than Soil Carbon Diffusion in Simulating Soil Carbon Profiles. *Journal of Geophysical Research: Biogeosciences, 126*(4), e2020JG006205. doi: 10.1029/2020jg006205.

Wardle, D. A., Bardgett, R. D., Klironomos, J. N., Set√§l√§, H., van der Putten, W. H., & Wall, D. H. (2004). Ecological Linkages Between Aboveground and Belowground Biota. *Science, 304*(5677), 1629-1633. doi: 10.1126/science.1094875.

Whalen, E. D., Grandy, A. S., Sokol, N. W., Keiluweit, M., Ernakovich, J., Smith, R. G., & Frey, S. D. (2022). Clarifying the evidence for microbial- and plant-derived soil organic matter, and the path toward a more quantitative understanding. *Glob Chang Biol, 28*(24), 7167-7185. doi: 10.1111/gcb.16413.

Wieder, W. R., Bonan, G. B., & Allison, S. D. (2013). Global soil carbon projections are improved by modelling microbial processes. *Nature Clim. Change, 3*(10), 909-912. doi: 10.1038/nclimate1951.

Wieder, W. R., Cleveland, C. C., Smith, W. K., & Todd-Brown, K. (2015). Future productivity and carbon storage limited by terrestrial nutrient availability. *Nature Geoscience, 8*(6), 441-444. doi: 10.1038/ngeo2413.

Wieder, W. R., Grandy, A. S., Kallenbach, C. M., & Bonan, G. B. (2014). Integrating microbial physiology and physio-chemical principles in soils with the MIcrobial-MIneral Carbon Stabilization (MIMICS) model. *Biogeosciences, 11*, 3899–3917. doi: 10.5194/bg-11-3899-2014.

Wieder, W. R., Grandy, A. S., Kallenbach, C. M., Taylor, P. G., & Bonan, G. B. (2015). Representing life in the Earth system with soil microbial functional traits in the MIMICS model. *Geoscientific Model Development, 8*(6), 1789-1808. doi: 10.5194/gmd-8-1789-2015.

Wieder, W. R., & Hartman, M. (2023). *Global MIMICS-CN from biogeochemical testbed*. doi: 10.5065/jqts-cg20.

Wieder, W. R., Hartman, M., Sulman, B., Kyker-Snowman, E., Eastman, B. A., & Wang, Y.-P. (2023). Soil Biogeochemical Testbed. Retrieved from https://github.com/wwieder/biogeochem_testbed. doi: 10.5281/zenodo.7636494.

Wieder, W. R., Hartman, M. D., Sulman, B. N., Wang, Y.-P., Koven, C. D., & Bonan, G. B. (2018). Carbon cycle confidence and uncertainty: Exploring variation among soil biogeochemical models. *Global Change Biology, 24*(4), 1563-1579. doi: 10.1111/gcb.13979.

Wieder, W. R., Sulman, B. N., Hartman, M. D., Koven, C. D., & Bradford, M. A. (2019). Arctic Soil Governs Whether Climate Change Drives Global Losses or Gains in Soil Carbon. *Geophysical Research Letters, 46*(24), 14486-14495. doi: 10.1029/2019gl085543.

Xu, X., Thornton, P. E., & Post, W. M. (2013). A global analysis of soil microbial biomass carbon, nitrogen and phosphorus in terrestrial ecosystems. *Global Ecology and Biogeography, 22*(6), 737-749. doi: 10.1111/geb.12029.

Xu, X., Thornton, P. E., & Potapov, P. (2014). *A Compilation of Global Soil Microbial Biomass Carbon, Nitrogen, and Phosphorus Data*. doi: 10.3334/ORNLDAAC/1264.

Yang, X., Ricciuto, D. M., Thornton, P. E., Shi, X., Xu, M., Hoffman, F., & Norby, R. J. (2019). The Effects of Phosphorus Cycle Dynamics on Carbon Sources and Sinks in the Amazon Region: A Modeling Study Using ELM v1. *Journal of Geophysical Research: Biogeosciences, 124*(12), 3686-3698. doi: 10.1029/2019jg005082.

Yue, K., Fornara, D. A., Yang, W., Peng, Y., Li, Z., Wu, F., & Peng, C. (2017). Effects of three global change drivers on terrestrial C:N:P stoichiometry: a global synthesis. *Glob Chang Biol, 23*(6), 2450-2463. doi: 10.1111/gcb.13569.

Zaehle, S., Friedlingstein, P., & Friend, A. D. (2010). Terrestrial nitrogen feedbacks may accelerate future climate change. *Geophysical Research Letters, 37*(1), L01401. doi: 10.1029/2009gl041345.

Zaehle, S., Jones, C. D., Houlton, B., Lamarque, J. F., & Robertson, E. (2015). Nitrogen Availability Reduces CMIP5 Projections of Twenty-First-Century Land Carbon Uptake. *Journal of Climate, 28*(6), 2494-2511. doi: 10.1175/Jcli-D-13-00776.1.

Zechmeister-Boltenstern, S., Keiblinger, K. M., Mooshammer, M., Peñuelas, J., Richter, A., Sardans, J., & Wanek, W. (2015). The application of ecological stoichiometry to plant–microbial–soil organic matter transformations. *Ecological Monographs, 85*(2), 133-155. doi: 10.1890/14-0777.1.

Zhang, H., Goll, D. S., Wang, Y.-P., Ciais, P., Wieder, W. R., Abramoff, R., Huang, Y., Guenet, B., Prescher, A.-K., Viscarra Rossel, R. A., Barré, P., Chenu, C., Zhou, G., & Tang, X. (2020). Microbial dynamics and soil physicochemical properties explain large-scale variations in soil organic carbon. *Global Change Biology, 26*(4), 2668-2685. doi: 10.1111/gcb.14994.

Zhang, Y., Lavallee, J. M., Robertson, A. D., Even, R., Ogle, S. M., Paustian, K., & Cotrufo, M. F. (2021). Simulating measurable ecosystem carbon and nitrogen dynamics with the mechanistically defined MEMS 2.0 model. *Biogeosciences, 18*(10), 3147-3171. doi: 10.5194/bg-18-3147-2021.

Zhu, Q., Riley, W. J., Tang, J., Collier, N., Hoffman, F. M., Yang, X., & Bisht, G. (2019). Representing Nitrogen, Phosphorus, and Carbon Interactions in the E3SM Land Model: Development and Global Benchmarking. *Journal of Advances in Modeling Earth Systems, 11*(7), 2238-2258. doi: 10.1029/2018ms001571.